University of Nevada, Reno

Modeling Capacity and Delay at Signalized Intersections with Channelized Right-turn Lanes Considering the Impact of Blockage

A dissertation submitted in partial fulfillment of the
requirements for the degree of Doctor of Philosophy in
Civil and Environmental Engineering

by

Saeedeh Farivar

Dr. Zong Tian/Dissertation Advisor

August, 2015

THE GRADUATE SCHOOL

We recommend that the dissertation
prepared under our supervision by

SAEEDEH FARIVAR

Entitled

**Modeling Capacity and Delay at Signalized Intersections with
Channelized Right-turn Lanes Considering the Impact of Blockage**

be accepted in partial fulfillment of the
requirements for the degree of

DOCTOR OF PHILOSOPHY

Zong Tian, Ph.D., Advisor

Reed Gibby, Ph.D., Committee Member

Hao Xu, Ph.D., Committee Member

Anna Panorska, Ph.D., Committee Member

Shunfeng Song, Ph.D., Committee Member

David W. Zeh, Ph.D., Dean, Graduate School

August, 2015

ABSTRACT

Right-turn channelization is used to improve the capacity at busy intersections with a lot of right-turns. However, under heavy traffic conditions the through lane vehicles might backup and block the right-turn lane. This will affect the discharge rate of right-turning vehicles and reduce the approach capacity and, consequently, increase the approach delay. So if the right-turn channelization is blocked frequently, its advantage is neglected and serious capacity problems can be overlooked. This issue is not addressed in the Highway Capacity Manual (HCM) and no separate model is provided to estimate the capacity and delay of approaches with channelized right-turn lanes. Using conventional methods for estimating the capacity and delay without considering the effect of potential blockage results in overestimation of the approach capacity and underestimation of the approach delay. This research presents probabilistic capacity and delay models for signalized intersections with channelized right-turn lanes considering the possibility of the right-turning vehicles being blocked from accessing the lane.

The capacity model was developed by considering the capacity under blockage and non-blockage conditions with respect to the probability of blockage. Subsequently, a model was developed to estimate the probability of blockage. The capacity model is significantly affected by the length of the short-lane section and proportion of right-turn traffic. The proposed capacity model under blockage conditions and also the blockage probability model were validated through VISSIM, a microscopic simulation model. The validation process showed that both models are reliable. For operational purposes, the recommended lengths of the short-lane section were developed which would be useful in

evaluating adequacy of the current lengths, identifying the options of extending the short-lane section length, or changing signal timing to reduce the likelihood of blockage. The recommended lengths were developed based on different signal timing plans and several proportions of right-turn traffic.

The queue accumulation polygons (QAPs) were used to estimate the approach uniform delay and the HCM procedure was followed for the computation of the incremental delay caused by the random fluctuation of vehicle arrivals. To investigate the effect of blockage on the uniform delay, two different QAPs were developed associated with arrival scenarios under blockage and non-blockage conditions. The proposed delay model was also validated through VISSIM. It was found that, the proposed model can provide accurate estimates of the delay by reflecting the delay increase due to the right-turn channelization blockage. The results showed that the delay of an approach with a channelized right-turn is influenced by the length of the short-lane section and proportion of through and right-turn traffic.

Keywords: Capacity, Delay, Signalized Intersections, Channelized Right-Turn Lane, Blockage, Residual Queue, Probability, Simulation

Dedicated to My Beloved Parents and My Husband

ACKNOWLEDGMENTS

TABLE OF CONTENTS

LIST OF TABLES

LIST OF FIGURES

CHAPTER 1: INTRODUCTION

1.1. BACKGROUND AND PROBLEM STATEMENT

Capacity and delay are two critical measures to evaluate the performance of signalized intersections. Capacity measures the intersection service rate while delay measures the quality of service. In the United States, the procedures provided in the Highway Capacity Manual (HCM) are widely used to estimate the capacity and delay of signalized intersections. However, HCM does not cover all intersection configurations including channelized right-turn lanes and right-turn-pockets.

Right-turn lanes separate the turning vehicles from through traffic and are used to improve the safety and operation of intersections. Several forms of right-turn lanes have been designed based on the geometry and right-turn control type. A common configuration of right-turn lane design is the channelized right-turn lane without the deceleration or acceleration lanes as depicted in Figure 1-1. Right-turn channelization is used at busy intersections with a lot of right-turns. It is used to improve capacity at such intersections by providing free-flow or nearly free-flow right-turn movements. By providing enough length of the short-lane section or storage length, right-turn traffic can be removed from the through traffic and can freely make a right-turn without incurring stops and delay caused by through traffic. However, under heavy traffic conditions, the through movement queue frequently block the throat of the right-turn lane and reduce the

capacity of the intersection. So if the right-turn channelization is blocked frequently, its advantage is neglected and serious capacity problems can be overlooked.
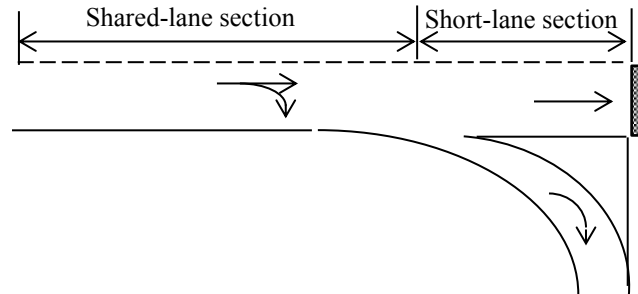
Figure 1-1. An Approach with a Channelized Right-Turn Lane

As Roess et al. (2004) stated, when right-turn channelization are added to an intersection, turning vehicles can be treated as if they do not use the intersection, so they do not affect the capacity and delay of the intersection. However, this concept is true only when traffic volumes are sufficiently light and through traffic do not interfere with right-turning vehicles. When the traffic demand is large, especially close to the capacity, and the length of the short-lane section is short, through vehicles will likely block the channelization entrance. Under this condition, some right-turn vehicles will become trapped by through vehicles preventing the right-turning vehicles from entering the right-turn channelization. Instead, they are delayed until the through vehicles ahead get discharged. This will affect the discharge rate of right-turn vehicles and reduce the approach capacity. Also, it will cause right-turn vehicles to experience an additional delay. This issue is not addressed in the current edition of HCM and in fact, HCM does not provide separate models to estimate the capacity and delay of signalized approaches with channelized right-turn lanes. Using the standard methods for estimating the capacity

and delay without considering the impact of blockage will lead to the overestimation of the approach capacity and underestimation of the approach delay.

Very few studies have focused on the performance of signalized intersections with channelized right-turn lanes while a blockage occurs (Macfarlane et al., 2011). Also, simulation models do not directly report the intersection and approach capacity, and because of significant variations involved in simulation, multiple runs are required to attain reasonable results (Tian et al., 2002). Therefore, it is desired to develop analytical models to estimate the approach capacity and delay considering the possibility and impact of blockage. By considering this effect, the proposed models can provide estimates of capacity and delay closer to practice than those provided by the conventional HCM models. In addition, investigating the effect of blockage and reviewing the through movement queue would be beneficial when establishing the length of short-lane section.

1.2. RESEARCH OBJECTIVES AND SCOPE

The main objective of this study is to model the capacity and delay of signalized approaches with channelized right-turn lanes under congested traffic conditions by considering the possibility of right-turn channelized lane blockage. More specifically, the probability of blockage will be calculated by taking into account the expected residual queue from the previous cycle. Any residual queue will lead to a higher probability of blockage, thus its determination is necessary to compute a more accurate blockage probability.

Based on the primary objective, the scope of this research includes:

- Identifying the possible scenarios of right-turn lane blockage,

- Estimating the probability of blockage to the right-turn channelization caused by through traffic,

- Estimating the expected residual queue from the previous cycle,

- Developing analytical capacity models consisting of capacities under blockage and non-blockage conditions,

- Developing analytical delay models considering the impact of blockage, and

- Using simulation models to calibrate and validate the proposed models.

1.3. RESEARCH PROCEDURES

According to the research objective and scope described in the previous section, this research was conducted following the steps below:

Step 1- Literature Review

Previous studies related to the following subjects were reviewed and evaluated:

- Capacity and delay estimates for signalized intersections,

- The impact of blockage on the intersection performance, and

- The appropriate lengths of turning bays considering the impact of blockage.

The comprehensive literature review documenting the existing studies related to the research topic provided a sufficient background and overview for the proposed study.

Step 2- Analytical Model Development and Calibration

In this research study, two proposed analytical models were the probabilistic capacity model and the Queue Accumulation Polygon (QPA) model to estimate the uniform approach delay under lane blockage and non-blockage conditions.

The proposed capacity model is estimated considering the probability of blockage with respect to the expected residual queue from the previous cycle. The capacity estimation procedure was as follows:

1) Identify all the possible queue patterns at the end of red phase,

2) Calculate the probability of each identified queue pattern and compute the probability that a blockage occurs by through vehicles to the right-turning vehicles,

3) Estimate the expected residual queue at the end of red phase,

4) Model the approach capacity under non-blockage condition,

5) Model the approach capacity under blockage condition,

6) Model the approach capacity considering blockage and non-blockage capacities and their corresponding probabilities,

7) Model the capacity for the approaches with more than one through lane by considering the through traffic distribution across the lanes, and

8) Calibrate the proposed models based on the results from the simulation models.

The QAPs were used to estimate the approach uniform delay. Different arrival patterns may occur after the onset of the red phase with some causing a blockage. Therefore, to investigate the impact of blockage on the approach uniform delay, two different QAPs were developed for the arrival scenarios associated with blockage and non-blockage conditions. The delay estimation procedure was as follows:

1) Identify the arrival scenarios associated with blockage and non-blockage conditions,

2) Construct the QAP for arrival scenarios leading to a non-blockage condition,

3) Construct the QAP for arrival scenarios leading to a blockage condition,

4) Develop the approach uniform delay for each arrival scenario based on their corresponding QAPs,

5) Calculate the approach uniform delay considering the corresponding probabilities of each arrival scenario,

6) Calculate the random delay term by following the HCM procedure, and

7) Model the delay for the approaches with more than one through lane by considering the through traffic distribution across the lanes.

Step 3- Proposed Model Validation Using Simulation

To evaluate the effectiveness of the proposed models in estimating the capacity and delay, the results from the proposed models were compared with the simulation outputs. Several simulation models were built to generate various scenarios of traffic conditions at an intersection with a channelized right-turn lane. In this study, VISSIM was chosen as the simulation tool.

After evaluating the effectiveness of the proposed model using simulation, the results are shown and the question of how blockage might influence the approach capacity and delay can be answered.

1.4. ORGANIZATION OF THE DISSERTATION

This dissertation consists of five chapters with the introduction as Chapter 1. Chapter 2 provides a comprehensive literature review on the estimation of capacity and delay at signalized intersections and also the estimation of blockage probability as well as the possibility of any residual queue. Chapters 3 and 4 are related to the proposed capacity and delay models, respectively. Conclusions and recommendations from this research are summarized in Chapter 5, which also provides suggestions for future research.

CHAPTER 2: LITERATURE REVIEW

2.1. INTRODUCTION

The primary objective of this study was to model the capacity and delay of signalized intersections with channelized right-turn lanes considering the impact of blockage. Most of the studies in the literature focused only on the queue length estimation to determine the appropriate storage lengths of the turning bays (Kikuchi et al. (2004), Kikuchi et al. (2007), Kikuchi and Kronprasert (2008, 2010), Qi et al. (2007)). These studies involved determining the probabilities of blockage and spillback with or without considering the residual queues. Only a few studies dealt with estimating the approach capacity and delay based on the probability of blockage. The results of these studies helped the author understand the interactions between through and right-turn vehicles under blockage conditions to investigate the approach capacity and delay using a probabilistic approach. In this regard, the reviewed studies focused on capacity and delay models for signalized intersections, application of blockage and spillback concept on capacity and delay estimations, and the appropriate lengths of turning bays.

2.2. CAPACITY AND DELAY MODELS FOR SIGNALIZED INTERSECTIONS

2.2.1. HCM Capacity Model

The Highway Capacity Manual (HCM 2010) is the most widely used guideline for

estimating the intersection capacity and delay. Chapter 18 of the manual provides a procedure for estimating the capacity and delay of lane groups at signalized intersections. Based on this procedure, the capacity of a lane group is obtained from the following equation:

$$c_i = s_i \frac{g_i}{C}$$

(2-1)

where,

- c_i is the capacity of lane group i (vph),

- s_i is the saturation flow rate for lane group i (vph), and

- $\frac{g_i}{C}$ is the effective green to cycle ratio for lane group i.

2.2.2. HCM Delay Model

Delay has been commonly defined as a form of stopped delay, control (signal) delay, travel-time delay, and queue delay. The intersection level of service (LOS) is determined based on the average control delay per vehicle which reflects the signal timing impacts on vehicles. In the HCM, the average control delay per vehicle for a given lane group is computed as a sum of three components: uniform delay, overflow delay, and initial queue delay as shown in Equation (2-2):

$$d = d_1 + d_2 + d_3$$

(2-2)

where,

- d is the control delay per vehicle (sec/veh),

- d_1 is the uniform delay assuming uniform arrivals (sec/veh),

- d_2 is the incremental delay to account for the effect of random arrivals and oversaturation queues (sec/veh). The incremental delay is derived assuming no initial queue at the start of the analysis period, and

- d_3 is the initial queue delay due to the initial queue at the start of the analysis period (sec/veh).

The formula for estimating the uniform delay can be derived from a plot of accumulated vehicles against time assuming uniform arrival and departure, no overflow queue, and no initial queues at the start of the red phase. As depicted in Figure 2-1.a, vehicles arrive at the uniform rate of V (vph) so that they start to accumulate and form the queue during the red interval. The discharge rate during the red interval is zero and after onset of the green interval, vehicles start to discharge from the queue at saturation flow rate of s (vph). After the queue is discharged, vehicles arrive and discharge at the same rate, V. Figure 2-1.b illustrates another form of uniform delay which leads to the same delay model as Figure 2-1.a. Figure 2-1.b shows the queue accumulation according to the vehicle arrivals as a function of time and is called queue accumulation polygon (QAP). The area of the polygon is the total delay.
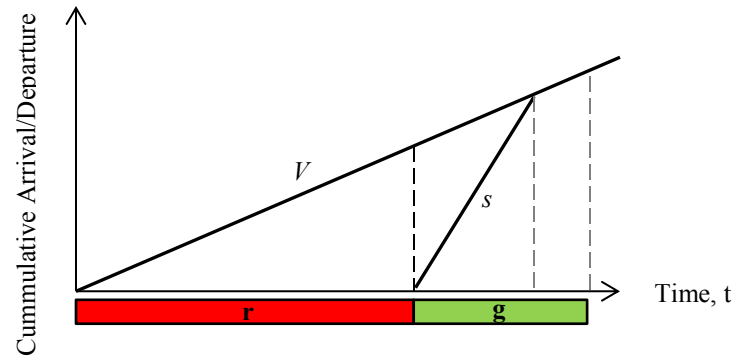
(a) Relationship between Arrivals, Departures, and Total Delay
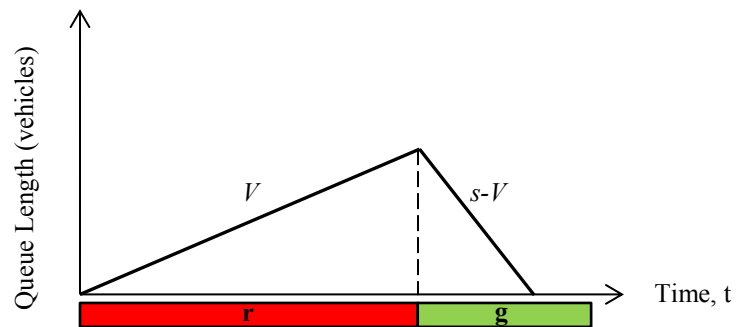
(b) Queue Accumulation Polygon (QAP)

Figure 2-1. An Illustration of Uniform Delay

The uniform delay is calculated as the area of a triangle formed by the arrival/departure curves shown in Figure 2-1:

$$d_1 = \frac{\frac{1}{2}C(1-\frac{g}{C})^2}{1-[\min(1,X)\frac{g}{C}]}$$

(2-3)

where,

- d_1 is the approach uniform delay (sec/veh),

- C is the cycle length (sec),

- g is the effective green time (sec),

- c is the lane group capacity (vph), and

- $X = \dfrac{V}{c}$ is the degree of saturation, $X \leq 1$.

For the signalized approaches with channelized right-turn lanes, HCM models are not adjusted to reflect the effect of through blockage on right-turn traffic. However, as mentioned in the introduction, during heavy traffic conditions the interactions between through and right-turn vehicles may result in different delays, particularly the uniform delay and the random delay which depend on the approach capacity. Using HCM models without considering the blockage effects, would lead to overestimation of the capacity and underestimation of the delay.

In the HCM, the random delay component is determined using Equation (2-4). This equation was derived by Fambro and Raphael (1997):

$$d_2 = 900T \left[(X_L - 1) + \sqrt{(X_L - 1)^2 + \frac{8kIX_L}{c_L T}} \right] \qquad (2\text{-}4)$$

where,

- T is the length of the analysis period (hour),

- c_L is the lane group capacity (vph) which is calculated using the proposed procedure in Chapter 3,

- X_L is the volume to capacity ratio equal to $\dfrac{V_L}{c_L}$,

- k is a factor that accounts for the effect of controller type on delay. A value of 0.50 is recommended for pre-timed phases which is the focus of this research, and

- I is the upstream filtering adjustment factor, which accounts for the effect of an upstream signal on vehicle arrivals to the study lane group. The value of this factor is 1.0 for an isolated intersection, which is a concern of this research.

The random delay term is valid for all degrees of saturation X_L including undersaturated and oversaturated conditions.

The random delay model is a time-dependent delay model, which was derived by using the "coordinate transformation" technique proposed by Whiting for the TRANSYT signal timing optimization program. The method was described in detail by Kimber and Hollis (1979). This technique transforms the steady-state function so that it is limiting to the deterministic queue model. This transformation is depicted in Figure 2-2.
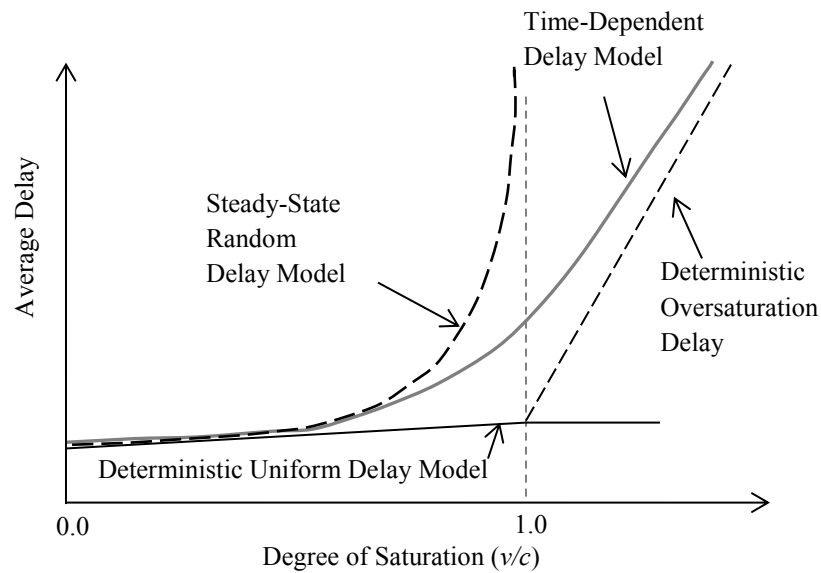
Figure 2-2. Coordinate Transformation

2.3. CAPACITY AND DELAY ESTIMATES BY CONSIDERING THE IMPACT OF BLOCKAGE AND SPILLBACK

Considering the blockage and spillback probabilities, only a few studies addressed the capacity and delay of signalized approaches influenced by turning movements. Tian and Wu (2006) developed a probabilistic capacity model for signalized intersections with a short right-turn lane. They modeled the approach capacity considering the impact of blockage on the right-turn lane caused by both overflowed right-turn and through vehicles. The capacity was found to be significantly affected by the length of the right-turn pocket, cycle length, and the proportion of right-tune vehicles. Through a general mathematical model, Wu (2011) studied the capacity reduction of a shared lane influenced by the permitted turning vehicles. By calculating the blockage probability, he proposed an exact mathematical model to estimate the capacity of single-shared lanes.

For practical applications, graphs were produced and approximation functions were provided to be easily applied and incorporated into the existing Germany Highway Capacity Manual. Zhang and Tong (2008) proposed a probabilistic capacity model for left-turn and through movements considering the probability of blockage and spillback. Their model provides acceptable results only for normal arrival rates since it does not account for the possibility of residual queues. They highlighted the impact of left-turn bay length and left-turn signal strategy on the capacity of signalized intersections. Their model was enhanced later by Osei-Asamoah et al. (2010), but its accuracy was still limited due to the issue of inter-cycle queue formation dependencies. In their study, capacity models were developed regarding left-turn spillover conditions by using a regression analysis over the simulation data. Their results showed significant improvement over HCM. Reynolds et al. (2011) developed a macroscopic simulation tool to quantify the impacts of short-turn pockets on the capacity of signalized intersections. They modeled the capacity reduction on multilane approaches using a series of flow and density restrictions on different regions of the approach. Although simulation models can be used to investigate the intersections capacity and delay, they do not directly report the intersection and approach capacities and delays and because of significant variations involved in simulation, multiple runs are required to get reasonable results (Tian et al., 2002).

Using the capacity results from Tian and Wu's (2006) study and considering the influence of blockage and spillback, Gao (2011) developed the uniform approach delay for signalized intersections with right-turn pockets. She also investigated the impact of

signal timing strategies on the right-turn delay. The delays were overestimated because of the assumption that a blockage happens in each cycle (100 percent of the time). The proposed delay models were calibrated against simulation using linear regression. Yin et al. (2012) developed probabilistic delay models for left-turn and through movements. For the leading left-turn operation, the left-turn delay model was developed by incorporating the impact of residual queues and blockage by through traffic. The through traffic delay then was modeled considering the left-turn spillback for a lagging protected left-turn operation. They used the Newell diffusion approximation technique (Newell, 1965) to estimate the expected residual queue. Their delay results were compared with those from the HCM model that does not reflect the blockage and spillback effects. They recommended their models to be replaced by the uniform delay term in the HCM under heavy traffic demand conditions.

There were only a few studies dealing specifically with channelized right-turn lanes like the study by Macfarlane et al. (2011) who focused only on the delay estimates of the right-turn channel. Using two real case studies, the authors showed that despite the existence of an acceleration auxiliary lane, right-turn vehicles unnecessarily hesitated in free right-turn lanes. This significantly increased their delay.

2.4. DETERMINING THE APPROPRIATE STORAGE LENGTH

In case of channelized right-turn lane without deceleration or acceleration lanes (as shown in Figure 1-1), there is a possibility of blockage happening at the beginning of the

turning lane. If the length of the short-lane section is not long enough, through vehicles that arrive in the red phase might overflow and block the right-turning vehicles from entering the lane. In this situation, the capacity of the lane group will be reduced: consequently, the delay will be increased. In the Policy on Geometric Design of Highways and Streets (AASHTO, 2011), the primary design elements of turning lane are the corner radius and lane width. No design guideline is provided to reflect the impact of blockage on the right-turn vehicles that are supposed to move freely. Therefore, the through movement queue should be reviewed and turning lanes should be designed such that no blockage occurs or occurs at a certain threshold.

Most of the studies in the literature focused on estimating the queue length and determining the appropriate storage lengths of the turning bays. These studies involved estimating the probability of blockage, spillback and/or residual queue. In some consecutive studies, Kikuchi et al. (2004, 2007) analyzed the lengths of turning lanes at signalized intersections taking into account the probabilities of blockage and spillback. In another study (Kikuchi and Kronprasert, 2008), they determined the appropriate length of right-turn lanes at signalized intersections for two timing strategies: right-turn on red (RTOR) permitted and not permitted. However, in their above mentioned studies, they did not consider the possibility of residual queue from the previous cycle for the through and turning lanes. In their most recent study (2010), Kikuchi and Kronprasert determined the lengths of left-turn lanes under different left-turn signal phasing schemes by considering the probability of leftover left-turn and through vehicles. Still, in the residual queue probability model, they did not consider the cycle-by-cycle dependency of the

queue formation so that a single cycle was modeled independently. Qi et al. (2007) considered the possibility of residual queues by applying the Discrete-Time Markov Chain (DTMC) model to determine the storage lengths of left-turn lanes at signalized intersections. Based on this procedure, which considers the overflow queue formation in a cycle-by-cycle basis, they found better estimates for the appropriate length of left-turn bays than any other existing methods.

2.4.1. Estimation of Overflow Queue

In undersaturated conditions, the overflow queues could form due to the random fluctuation in arrival flow rates, which result in oversaturated conditions in some cycles. However, since the overall arrival flow rate is below the capacity, this situation will last for a finite period of time and overflow queues will be discharged in subsequent cycles. Yin et.al (2012) applied Newell's method in their study to estimate the expected residual queue. Newell's method is one of the early models of overflow queue at pre-timed traffic signals under the assumption of stationary arrivals and departures. These models, called steady-state models, are applicable only to undersaturated conditions so that they predict infinite queues for saturated conditions when the demand gets close to the capacity (volume to capacity ratio=$X \sim$). As Olszewski (1990) mentioned, during a finite period of peak traffic flow, the queue can only grow to a finite size. The limitation of steady-state models in estimation of the overflow queue for flows near capacity led to the development of time-dependent models by applying the method of coordinate transformation. This technique transforms the undersaturated (steady-state) function to the oversaturated function and provides queue overflow results applicable to both

conditions. The coordinate transformation approach inspired Akcelik to derivate a time-dependent overflow queue. He developed a transition function for the average overflow queue to be incorporated in HCM 2000 (Akcelik, 1998):

$$Q_2 = 0.25c_L T \left[(X_L - 1) + \sqrt{(X_L - 1)^2 + \frac{8k_B X_L}{c_L T} + \frac{16k_B Q_{bL}}{(c_L T)^2}} \right] \qquad (2\text{-}5)$$

where,

- Q_2 is an estimate for average residual queue (vehicles),

- T is the length of the analysis period (hour),

- c_L is the lane group capacity (vph),

- X_L is the volume to capacity ratio equal to $\dfrac{V_L}{c_L}$,

- k_B is the adjustment factor related to early arrivals; $k_B = 0.12I \left(\dfrac{s_L g}{3600} \right)^{0.7}$,

- I is the upstream filtering factor for platoon arrivals (I is equal to one for isolated intersections as the case of this study),

- s_L is the lane group saturation flow rate per lane (vph),

- Q_{bL} is the initial queue (vehicles) at the start of analysis period which was assumed to be zero in this study.

The above equation predicts non-zero overflow queues for all degrees of saturation.

Figure 2-3 shows how the time-dependent model transforms the steady-state function so that it is limiting to the deterministic queue model for oversaturated conditions. As can be seen in this figure, neither steady-state function nor deterministic oversaturation function gives reasonable results for flows near capacity (Akcelik, 2011).
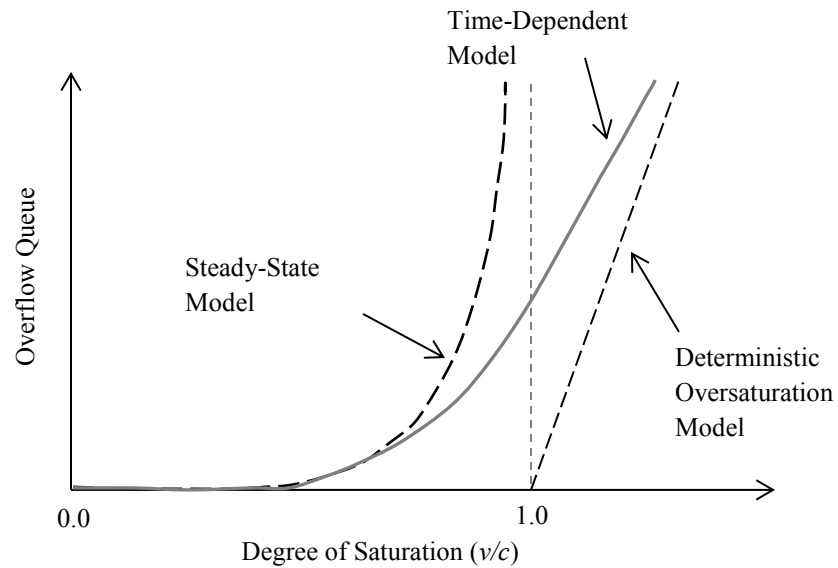
Figure 2-3. The Relationship between the Steady-State, Deterministic Oversaturation, and Time-Dependent Models for Overflow Queue Estimation

CHAPTER 3: MODELING RIGHT-TURN BLOCKAGE AND APPROACH CAPACITY

3.1. INTRODUCTION

When the traffic demand is high, especially close to the capacity, through movement queue overflow may result in right-turn blockage, especially when the short-lane section is short. This will affect the discharge rate of right-turn vehicles and reduce the approach capacity. This issue is not addressed in the HCM and in fact, HCM does not provide a separate method to estimate the capacity of a signalized approach with a channelized right-turn lane. Using the standard methods for estimating the capacity without considering the possibility of blockage would lead to the overestimation of the approach capacity and underestimation of the approach delay. Therefore, this chapter introduces a capacity model for a pre-timed signalized approach with a channelized right-turn lane by considering the probability of blockage. More specifically, the probability of blockage was calculated with respect to the expected residual queue from the previous cycle. The capacity model derivation involved three major steps: (1) Calculating the probability of blockage to the right-turn channel caused by through traffic, (2) Calculating the expected number of left-over through vehicles from the previous cycle as the through residual queue, and (3) Modeling the approach capacity under both blockage and non-blockage conditions.

3.2. PROBABILITY OF BLOCKAGE

The probability of blockage was defined as the probability that the channel throat is blocked by through vehicles in a cycle. In the case of multiple through lanes, the traffic distribution between lanes is affected so that less through vehicles may use the rightmost lane. To develop the blockage probability model, length of the short-lane section was assumed to store N vehicles as depicted in Figure 3-1, so right-turning vehicles following N^{th} through vehicle were able to get into the right-turn channel.
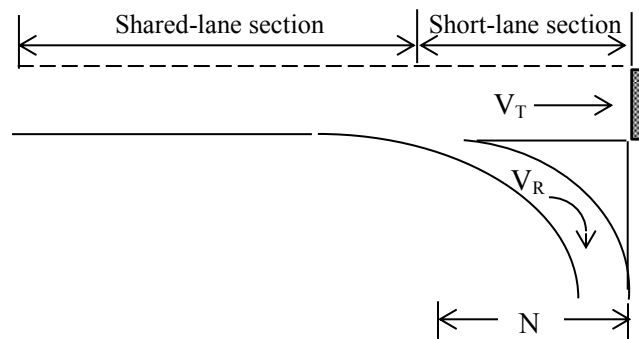
Figure 3-1. Elements of an Approach with Channelized Right-turn Lane

3.2.1. Possible Queue Patterns and Their Probabilities at the End of Red Interval

According to Figure 3-1, three different queue patterns could happen at the end of red interval as illustrated in Figure 3-2.

Pattern 1- Non Blockage. No through vehicles overflow so that the number of through vehicles that arrive during the red interval is less than $N+1$.

Pattern 2- Acceptable Blockage. Through vehicles overflow but no right-turn blockage occurs. All the right-turn vehicles arrive before $(N+1)^{th}$ through vehicle or before blockage occurs.

Pattern 3- Unacceptable Blockage. Some right-turn vehicles arrive after the arrival of $(N+1)^{th}$ through vehicle.

The occurrence probability of each pattern can be determined through three calculation steps:

Step 1 – $P(X_T, X_R)$, the probability that X_T through vehicles and X_R right-turn vehicles arrive during the red interval and before starting the green interval.

Step 2 – $P(Pattern\ \ i\,|\,(X_T, X_R))$, the probability that pattern i occurs when (X_T, X_R) are present.

Step 3 – $P(Pattern\ \ i)$, the probability that pattern i occurs for all combinations of (X_T, X_R).

In the following, the calculation process of occurrence probability for each step is discussed.

Step 1 – $P(X_T, X_R)$:

Assuming the arrival of through and right-turn vehicles during the red interval as independent events, the probability that X_T through vehicles and X_R right-turn vehicles arrive can be obtained as follow:

$$P(X_T, X_R) = P(X_T)P(X_R) \tag{3-1}$$

Since an isolated intersection is concerned, the arrival pattern of vehicles was assumed to be random following Poisson distribution. Hence,

$$P(X_T, X_R) = P(X_T)P(X_R) = \frac{(\lambda_T)^{X_T} e^{-\lambda_T}}{X_T!} \frac{(\lambda_R)^{X_R} e^{-\lambda_R}}{X_R!} \tag{3-2}$$

The average numbers of through and right-turn vehicles that arrive in red are

$\lambda_T = \dfrac{V_T * r}{3600}$ and $\lambda_R = \dfrac{V_R * r}{3600}$, respectively.

where,

- V_T is the approach average through volume (vph),

- V_R is the approach average right-turn volume (vph), and

- r is the effective red time (sec),

Step 2 – $P(Pattern \quad i \,|\, (X_T, X_R))$:

The probability that queue pattern i occurs when (X_T, X_R) are present, can be determined as the ratio of the number of sequences of vehicles resulting in that pattern and the number of all possible sequences.

$$P(Pattern \quad i | (X_T, X_R)) = \frac{no. \quad of \quad possible \quad vehicle \quad sequence \quad in \quad pattern \quad i}{no. \quad of \quad all \quad possible \quad vehicle \quad sequence \quad for \quad all \quad (X_T, X_R)} \tag{3-3}$$

For example, in pattern 2, the number of combinations that X_R right-turn vehicles arrive before the $(N+1-E(q))^{th}$ through vehicle, which blocks the channel entrance, is $_{N+1-E(q)+X_R}C_{X_R}$, and the number of all possible sequences with $X_T - E(q)$ through vehicles and X_R right-turn vehicles is $_{X_T-E(q)+X_R}C_{X_R}$, where, $E(q)$ is the expected residual queue on the through lane at the beginning of the red interval. Thus, the probability of pattern 2 is:

$$P(Pattern \quad 2 \mid (X_T, X_R)) = \frac{_{N+1-E(q)+X_R}C_{X_R}}{_{X_T-E(q)+X_R}C_{X_R}} \tag{3-4}$$

$$_{N-E(q)+X_R}C_{X_R} = \binom{N+1-E(q)+X_R}{X_R} = \frac{(N+1-E(q)+X_R)!}{X_R!(N-E(q))!} \tag{3-5}$$

$$_{X_T-E(q)+X_R}C_{X_R} = \binom{X_T-E(q)+X_R}{X_R} = \frac{(X_T-E(q)+X_R)!}{X_R!(X_T-E(q))!} \tag{3-6}$$

Assuming $E(q)$ as the expected residual queue on the through lane at the end of the green interval, arrival of only $(N-E(q))$ through vehicles is needed for causing a blockage. The estimation of expected residual queue is discussed later in this chapter.

Step 3 – $P(Pattern \quad i)$:

The probability of each pattern for all possible (X_T, X_R) combinations was obtained as provided in Equation (3-7):

$$P(Pattern \quad i) = \sum_{X_T}\sum_{X_R} P(X_T, X_R) \times P(Pattern \quad i \mid (X_T, X_R)) \tag{3-7}$$

For the previous example, the probability of pattern 2 for all (X_T, X_R) is:

$$P(Pattern\quad 2) = \sum_{X_T=N+1-E(q)}^{a_T^{max}} \sum_{X_R=0}^{a_R^{max}} P(X_T,X_R) \times P(Pattern\quad 2\,|\,(X_T,X_R)) \qquad (3\text{-}8)$$

$$P(Pattern\quad 2) = \sum_{X_T=N+1-E(q)}^{a_T^{max}} \sum_{X_R=0}^{a_R^{max}} \frac{(\lambda_T)^{X_T} e^{-\lambda_T}}{X_T!} \frac{(\lambda_R)^{X_R} e^{-\lambda R}}{X_R!} \times \frac{\binom{N+1-E(q)+X_R}{X_R}}{\binom{X_T-E(q)+X_R}{X_R}} \qquad (3\text{-}9)$$

In Equations (3-8) and (3-9):

- a_T^{max} is the maximum number of through vehicles that could arrive in a cycle, and

- a_R^{max} is the maximum number of right-turn vehicles that could arrive in a cycle.

They were determined as 95th percentiles of the number of arrivals. In the other words, no more than a_T^{max} through and a_R^{max} right-turn vehicles arrives 95 percent of the times or during 95 percent of cycles in an hour. The probability of each queue pattern according to the vehicle arrivals and sequences is shown in Figure 3-2.

Among the three queue patterns, pattern 1 and 2 were considered as non-blockage conditions so their probabilities were added and called the probability of non-blockage. Only pattern 3 was considered as the blockage condition. A numerical example representative of the proposed procedure is found in Appendix A.
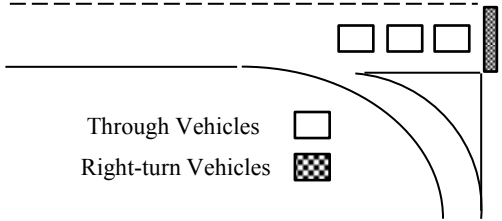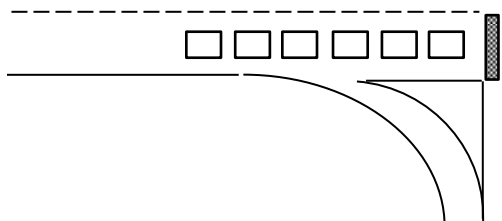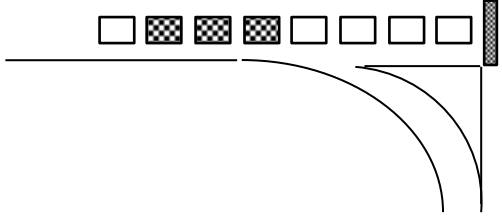
Condition	Pattern No.	Queue Patterns of (X_T, X_R)	Probability, $P(Pattern\ i)$
Non-blockage	1- No Blockage	Through Vehicles ☐ Right-turn Vehicles ▦	$$\sum_{X_T=0}^{N+1-E(q)} \sum_{X_R=0}^{a_R^{max}} \frac{(\lambda_T)^{X_T} e^{-\lambda_T}}{X_T!} \frac{(\lambda_R)^{X_R} e^{-\lambda_R}}{X_R!}$$
	2- Acceptable Blockage		$$\sum_{X_T=N+1-E(q)}^{a_T^{max}} \sum_{X_R=0}^{a_R^{max}} \frac{(\lambda_T)^{X_T} e^{-\lambda_T}}{X_T!} \frac{(\lambda_R)^{X_R} e^{-\lambda R}}{X_R!} \times \frac{\binom{N+1-E(q)+X_R}{X_R}}{\binom{X_T-E(q)+X_R}{X_R}}$$
Blockage	3- Unacceptable Blockage		$$\sum_{X_T=N+1-E(q)}^{a_T^{max}} \sum_{X_R=0}^{a_R^{max}} \frac{(\lambda_T)^{X_T} e^{-\lambda_T}}{X_T!} \frac{(\lambda_R)^{X_R} e^{-\lambda R}}{X_R!} \times \left[1 - \frac{\binom{N+1-E(q)+X_R}{X_R}}{\binom{X_T-E(q)+X_R}{X_R}} \right]$$

Figure 3-2. Possible Queue Patterns at the End of Red Interval and their Probabilities, *P(Pattern i)*

3.2.2. Estimation of Expected Residual Queue at the end of Green Interval (*E(q)*)

As discussed in the previous section, the probability of blockage is calculated by incorporating the influence of residual queues. Although residual queue is mostly observed in oversaturated conditions, it might be observed in under-saturated conditions especially when the traffic volume is close to the capacity. Under heavy traffic conditions, due to the random fluctuations in traffic demand, some through vehicles may not be served during some cycles, resulting in residual queues at the beginning of the red interval. A residual queue may be carried out from one cycle to the next cycle and cause higher probability of blockage occurring in the next cycle. Therefore, an accurate estimation of the residual queue is necessary. In this study, two methodologies were adopted to estimate the expected residual queue and then their results were compared and validated through simulation. One methodology is the Discrete-time Markov Chain (DTMC) method applied by Qi et al. (2007) to determine the probability of residual queues and consequently, the expected residual queue. The other methodology is the HCM methodology which estimates the residual queue as the second term of the average back-up queue.

Discrete-time Markov Chain (DTMC)

The cycle-to-cycle queue formation dependency can be modeled using the DTMC model in which the state of the next point depends only on the state of the current point. In estimating the probability of residual queue, it is reasonable to use this method because the queue at the end of the next green interval will depend on the queue at the end of the current green interval.

For the DTMC, it is important to first derive the one-step transition matrix P as is shown in Figure 3-3. In this figure, i and j which show the numbers in rows and columns, represent the residual queue of the current and the next cycle, respectively.

	0	1	2	....	j	....	φ
0	p_{00}	p_{01}	p_{02}	....	p_{0j}	....	
1	p_{10}	p_{11}	p_{12}	....	p_{1j}	....	
2	p_{20}	p_{21}	p_{22}	....	p_{2j}	....	
⋮						....	
i	p_{i0}	p_{i1}	p_{i2}	....	p_{ij}	....	
⋮						....	
m	p_{m0}	p_{m1}	p_{m2}	....	p_{mj}	....	
m+1	0	$p_{m+1,1}$	$p_{m+1,2}$	....	$p_{m+1,j}$	....	
m+2	0	0	$p_{m+2,2}$	....	$p_{m+2,j}$	....	
⋮	0	0	0				
φ							

Figure 3-3. DTMC One-Step Transition Matrix P

In matrix P, p_{ij} is the probability that the residual queue is i at the current cycle and becomes j at the next cycle. Assuming the stationary arrivals and constant departures, p_{ij} can be determined for three different parts of the matrix as follows:

1) When $j = 0$, or all the vehicles in queue in the current cycle are discharged at the end of the green interval of the next cycle. Considering m as the approach service rate and i as the left-over queue length in the current cycle, to clear all the vehicles in the next cycle, the number of arrivals plus the existing queue should be less than the capacity. Therefore, p_{ij} is calculated as:

$$p_{ij} = P(\text{arrivals in cycle}, k \leq \text{capcity} - i) = \sum_{k=0}^{m} \frac{\lambda^k e^{-\lambda}}{k!}, \qquad 0 < m - i \leq a_T^{\max} \qquad (3\text{-}10)$$

where, k is the number of arrivals in a cycle, and λ is the average number of through vehicles that arrive in a cycle, $\lambda = \dfrac{V_T * C}{3600}$.

2) When $j > 0$, or a residual queue is carried out to the next cycle. To have j vehicles as the residual queue in the next cycle, the number of arrivals plus the existing queue should be equal to the capacity plus j, so:

$$p_{ij} = P(\text{arrivals in cycle}, k = \text{capcity} + j - i) = \frac{\lambda^{m+j-i} e^{-\lambda}}{(m+j-i)!}, \qquad 0 \leq m - i + j \leq a_T^{\max} \qquad (3\text{-}11)$$

3) Otherwise, $p_{ij} = 0$.

In Equations (3-10) and (3-11), the capacity m is the maximum number of through vehicles that can be discharged in each cycle depending on the effective green time g, and the saturation headway T as follows:

$$m = \frac{g}{T} \qquad (3\text{-}12)$$

The typical value for the saturation headway of the through movement is 2 seconds. However, as it is discussed later in the calibration process, the through movement saturation headway was found to be 1.74 seconds, so $T=1.74$sec.

In determining the dimension of matrix P ($\varphi \times \varphi$), φ should be large enough so that the probability of the residual queue greater than φ becomes close to zero. In this research, the 95th percentile of the queue length was calculated and considered as the

upper bound of the residual queue. The 95th percentile of the queue length was obtained using a formula provided in the Traffic Signal Timing Manual (2008) as follows:

$$\varphi = Q_{95^{th}} = 2 \times Q_{average} = 2 \times \frac{V_T}{3600/(C-g)}$$ (3-13)

Thus, the one-step transition matrix P becomes a $\varphi \times \varphi$ matrix with the elements

$$p_{i\varphi} = 1 - \sum_{j=0}^{\varphi} pij \ .$$

In an n-step transition probability with sufficiently large n, the probabilistic behavior of the Markov chain becomes independent of the starting state. The stationary probability distribution π of the DTMC can be obtained as the limit of P^n when n is sufficiently high ($p_{ij}^n \rightarrow \pi_j$), where π_j represents the stationary probability of j vehicles left over at the end of the green interval.

$$\pi_j = P(Residual \ queue \ = j) \qquad j = 0,1,...,\varphi$$ (3-14)

By having the probability distribution of the residual queue, the following equation was used as an approximation to determine the expected residual queue required to calculate the blockage probability.

$$E(q) = \sum_{q=0}^{1-\phi} q\pi_q$$ (3-15)

HCM Average Residual Queue Estimation

The HCM formula as shown in Equation (3-16), can be used as an approximation of the cycle residual queue.

$$E(q) = Q_2 = 0.25c_L T \left[(X_L - 1) + \sqrt{(X_L - 1)^2 + \frac{8k_B X_L}{c_L T} + \frac{16k_B Q_{bL}}{(c_L T)^2}} \right] \qquad (3\text{-}16)$$

where,

- Q_2 is the second term of queued vehicles, an estimate for average residual queue (vehicles),

- T is the length of the analysis period (hour),

- c_L is the lane group capacity (vph),

- X_L is the volume to capacity ratio equal to $\dfrac{V_L}{c_L}$,

- k_B is the adjustment factor related to early arrivals, and

- Q_{bL} is the initial queue at the start of analysis period which is assumed to be zero in this study.

Since pre-timed signals are the topic of this study, the adjustment factor related to early arrivals was calculated as follows (HCM 2000):

$$k_B = 0.12I \left(\frac{s_L g}{3600} \right)^{0.7} \qquad (3\text{-}17)$$

where,

- I is the upstream filtering factor for platoon arrivals (I is equal to 1.0 for isolated intersections as the case of this study), and

- s_L is the lane group saturation flow rate per lane (vph).

The lane group capacity used in Equation (3-16) should be the capacity of the through movement. Although the study lane group is a shared lane, the random fluctuation of only through traffic could result in residual queues at the end of the green interval. With this consideration, the through movement capacity was assumed not to be influenced by blockage. This was a reasonable assumption because a blockage was defined as the condition when through vehicles overflow and block the channel entrance, so only right-turn movement capacity is affected by the blockage. Thus, the lane group capacity for use in Equation (3-16) can be obtained as follows:

$$c_L = \frac{g}{C} s_N \qquad (3\text{-}18)$$

where, s_N is the saturation flow rate from the shared lane section (vph).

3.3. PROPOSED CAPACITY MODEL

The capacity derivation process included estimation of capacity under two conditions: one was the approach capacity under blockage condition and the other one was the approach capacity under non-blockage condition. First, they were modeled separately and then the blockage and non-blockage probabilities were applied to obtain the total approach capacity. To derive the approach capacity model, the following assumptions were made:

a) First, a pre-timed signalized approach was assumed to include one through lane so the blockage and non-blockage capacities were estimated for this case. For the case of multiple through lanes, the capacity was estimated for each lane group by making an adjustment on the lane utilization factor.

b) Through traffic demand was assumed to be high enough to cause blockage at some cycles at the start of the green interval.

c) The length of the right-turn channel was assumed to be long enough to avoid queue spillback to the channel throat.

d) All the vehicles were assumed to be passenger cars.

3.3.1 Capacity under Non-Blockage Condition

In non-blockage condition, the approach can be treated as a shared lane with assuming that the right-turn vehicles can get into the channel during the red interval. Therefore, the approach capacity under non-blockage condition was determined to discharge vehicles during two time intervals: the green interval for discharging both through and right-turn vehicles, and the red interval for discharging only right-turn vehicles:

$$c_{non-block} = \frac{g}{C} s_N + \frac{r}{C} s_R \tag{3-19}$$

where,

- g is the effective green time (sec),

- r is the effective red time (sec),

- C is the cycle length (sec),

- s_N is the saturation flow rate from the shared lane section (vph), and

- s_R is the right-turn saturation flow rate (vph).

3.3.2. Capacity under Blockage Condition

At a signalized intersection with a channelized right-turn lane, right-turning vehicles can make a turn during both green and red intervals. However, when through vehicles overflow and blockage occurs after the onset of the red interval, the discharge rate of right-turn vehicles will depend on the arrival rate of through vehicles and the length of the short-lane section.

The approach capacity under blockage condition was determined based on discharging flow during three consecutive time intervals. The first interval starts right after the onset of the green interval during which only through vehicles in the short-lane section clear the approach. At the end of this interval, the blockage disappears. During the remaining green time, both through and right-turn vehicles depart from the shared lane section. During the third interval, which starts at the onset of the red interval, right-turn vehicles can go through the channel until through vehicles overflow and block the channel throat. The final approach capacity under blockage condition is the summation of all capacities calculated in these three time intervals.

As mentioned in section 3.2, a blockage occurs at the arrival of $(N+1)^{th}$ through vehicle. With this consideration, the first portion of green time is to discharge $(N+1)$ through vehicles from the short-lane section. Hence, the first part of capacity is:

$$c_1 = \frac{3600}{C}(N+1)$$ (3-20)

The required green time for discharging $(N+1)$ vehicles can be obtained as follows:

$$g_1 = \frac{(N+1)}{s_T}3600 + t_s$$ (3-21)

where,

- s_T is the saturation flow rate of the through movement (vph), and

- t_s is the start-up lost time (sec).

During the remaining portion of the green time, both through and right-turn vehicles depart from the shared lane section with the saturation flow rate of the shared lane, s_N. Therefore, the second part of capacity can be calculated using Equation (3-22):

$$c_2 = \left(\frac{g - g_1}{C}\right)s_N$$ (3-22)

The last portion of the capacity under blockage conditions is the average number of right-turn vehicles that can make a right-turn after onset of the red interval and prior to the blockage occurrence. By the time that the blockage occurs, $(N+1)$ through vehicles have arrived and stopped before the stop bar. During this time, the number of discharged

right-turn vehicles will depends on the proportion of right-turn to through vehicles so its capacity is obtained as follows:

$$c_3 = \frac{V_R}{V_T}\left(\frac{3600}{C}\right)(N+1) \qquad (3\text{-}23)$$

The total approach capacity under blockage condition is the sum of through and right-turn capacities obtained from Equations (3-20), (3-22), and (3-23) as follows:

$$c_{block} = c_1 + c_2 + c_3 = \frac{3600}{C}(N+1)\left(1+\frac{V_R}{V_T}\right) + \frac{g-g_1}{C}s_N \qquad (3\text{-}24)$$

Considering the probability of blockage which is obtained from section 3.2., the total approach capacity is calculated using the following equation:

$$c = P_{block}c_{block} + (1 - P_{block})c_{non-block} \qquad (3\text{-}25)$$

A numerical example of the aforementioned procedure can be found in Appendix A.

3.3.3. Capacity of Multilane Approach

In the case of multiple through lanes, one lane group can be associated with the rightmost through lane treated as a shared lane. The capacity of this shared lane was provided in the previous section. The other lane group can be associated with the remaining through lanes. The final approach capacity would be the summation of capacities of all the lane groups as follows:

$$c_{approach} = c_{lane1} + c_{lane2} = c + (n-1)\frac{g}{C}s_T \qquad (3\text{-}26)$$

where, c is the capacity of the rightmost lane, which is obtained using Equation (3-25), and n is the number of lanes.

To obtain the lane group capacities, the lane utilization or the traffic distribution across the lanes needs to be determined by considering the impact of blockage. To calculate the probability of blockage and the capacity of the rightmost through lane, the estimation of through traffic departing from the rightmost lane was necessary. In this study, the methodology proposed by Tarko (2007) was adopted in which the through traffic using the rightmost lane is treated as the impeding volume to the vehicles making a right turn on red (RTOR) from the approach located to the right of through vehicles' approach. The following section provides the details of this methodology.

Through Traffic Distribution across the Lanes

The amount of through traffic that uses the rightmost lane depends on the total traffic volume of the approach and the length of the short-lane section. For example, when right-turn volume is heavy and the short-lane section is very short, through vehicles may be discouraged to use the rightmost shared lane. In another case, a long short-lane effectively removes right-turn vehicles from the rightmost lane much further from the stop bar, thus through traffic is more uniformly distributed across all the lanes. Figure 3-4 illustrates an example of traffic distribution between two lanes where through vehicles are uniformly distributed between lanes from the stop bar to the channel throat, beyond which some right-turn vehicles are blocked and mixed in the queue. Based on Tarko's idea, the through traffic V_i, using the rightmost lane can be approximated by the following equation:

$$V_i = Nm + \frac{(V_T - Nmn) + (V_R - bm)}{n} - (V_R - bm) \tag{3-27}$$

where,

- m is number of cycles in one hour,

- n is the number of lanes,

- N is length of the short-lane section,

- b is number of right-turn vehicles have already passed through the channel during red interval,

- V_R is the right-turn volume, and

- V_T is the through volume.

The first term of Equation (3-27), Nm is the portion of through traffic that forms the queue at the rightmost lane up to the right-turn channel. The second term is the remainder of traffic flow in the rightmost lane, and $(V_R - bm)$ is the portion of right-turn traffic that could not leave the rightmost lane during the red interval. The components of Equation (3-27) are shown in in Figure 3-4.
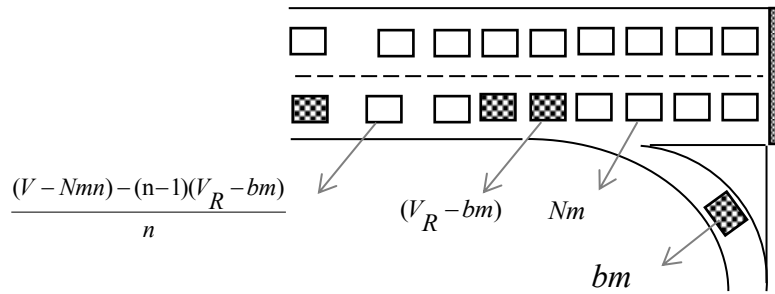
Figure 3-4. Distribution of Vehicles Across the Lanes

The second term of Equation (3-27) was obtained with the assumption of uniform distribution of traffic beyond the channel throat. This traffic does not include the through vehicles from the stop bar to the channel throat (Nmn), and also the right-turn vehicles that have already passed across the channel during red (bm). The assumption of uniform distribution is valid if the through traffic is high enough to use the rightmost lane despite the presence of right-turn vehicles, so:

$$\frac{V_T - Nmn}{n-1} > V_R - bm \tag{3-28}$$

If the through traffic flow is weaker, the queue beyond the channel throat will consist of only right-turn vehicles. Therefore, the through traffic using the rightmost lane includes only the vehicles queued up to the channel throat as follows:

$$V_i = Nm \tag{3-29}$$

For the very long short-lane sections, Equation (3-28) may result in a skewed volume distribution so that most of through vehicles use the rightmost lane. When the short-lane section is large enough, there is a smaller chance of blockage so through vehicles are

uniformly distributed between lanes. To prevent this skewness in the volume distribution, Equation (3-29) was modified as follows:

$$\begin{cases} V_i = Nm & if \quad V_i \le 0.5V_T \\ V_i = 0.5V_T & otherwise \end{cases} \tag{3-30}$$

This condition assured the uniform volume distribution for the cases of longer short-lane sections. As shown later in the validation process, the probability of blockage for these cases is less than 10 percent so the volume distribution is uniform and independent from the short-lane section length and traffic volume.

In the case of multiple through lanes, V_i was used as the through volume in sections 3.2 and 3.3 to calculate the probability of blockage and consequently, the capacity of the rightmost lane group.

Estimation of the Average Number of Unblocked Right-turn Vehicles in Red, b

During the red interval, right-turn vehicles can get through the channel under two conditions; one is under non-blockage condition when the number of through arrivals on red is less than $(N+1)$, and the other one is under blockage condition when some right-turn vehicles arrive before the $(N+1)^{th}$ through vehicle.

In the first situation, the number of unblocked right-turn vehicles x can be considered as a result of t independent experiments (total number of arrivals in red at the rightmost lane) with the probability of success p_r (proportion of right turns in the rightmost lane). The binomial distribution is used to calculate the probability $P_B(x)$ that x right-turn vehicles are not blocked:

$$P_B(x) = \binom{t}{x} p_r{}^x (1 - p_r)^{t-x} \tag{3-31}$$

In this case, the number of through vehicles t-x is less than $(N+1)$, which means $x > t - (N+1)$.

In the second situation, the probability that x right-turn vehicles arrive before $(N+1)^{th}$ through vehicle, can be obtained using the negative binomial distribution. In this case, the number of unblocked right-turn vehicles, x, is the number of failures before $(N+1)^{th}$ success:

$$P_{NB}(x) = \binom{x+N}{N} (1 - p_r)^N p_r{}^x \tag{3-32}$$

Considering both situations and their probabilities, the average value of x was then calculated as follows:

$$b = \sum_{x=0}^{t-(N+1)} x.P_B(x) + \sum_{t-N}^{t} x.P_{NB}(x) \tag{3-33}$$

Based on Tarko's work, the following equation can be used as an approximation of Equation (3-33) to estimate b if one of the above mentioned distributions prevails.

$$b = \min\{p_r.(N+1)/(1-p_r), p_r.t\} \tag{3-34}$$

Assuming that the through vehicles are distributed equally between all the lanes, the expected number of vehicles that would arrive on the approach at the rightmost lane in red can be obtained as follows:

$$t = \frac{a_T}{n} + a_R \qquad\qquad (3\text{-}35)$$

where, a_T and a_R are the expected numbers of through and right-turn arrivals during the red interval, respectively.

3.4. MODEL CALIBRATION AND VALIDATION

The model validation process consisted of four parts; first, validating the blockage probability model developed in Section 3.2.; second, validating the proposed capacity model under blockage condition; third, validating the traffic distribution model (Tarko's model); and finally, validation of the proposed capacity model under blockage condition for the case of two-lane approach.

To evaluate the accuracy of the proposed models, a set of simulation experiments were conducted in VISSIM. To be consistent with the proposed models, a pre-timed signalized intersection was modeled in VISSIM and all the vehicles were assumed to be passenger cars. It was also assumed that the right-turning vehicles can merge into the traffic flow by yielding to oncoming vehicles so that no right-turn spillback occurs. The site characteristics of the study intersection are shown in Figure 3-5. The eastbound approaches with one and two through lanes and different lengths of the short-lane section were the study approaches.
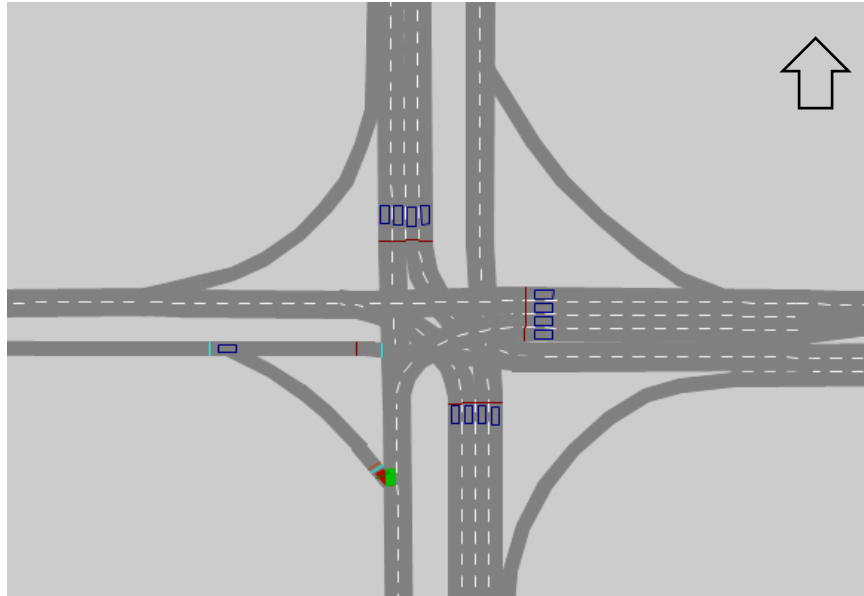
a) Eastbound Approach with Single Through Lane
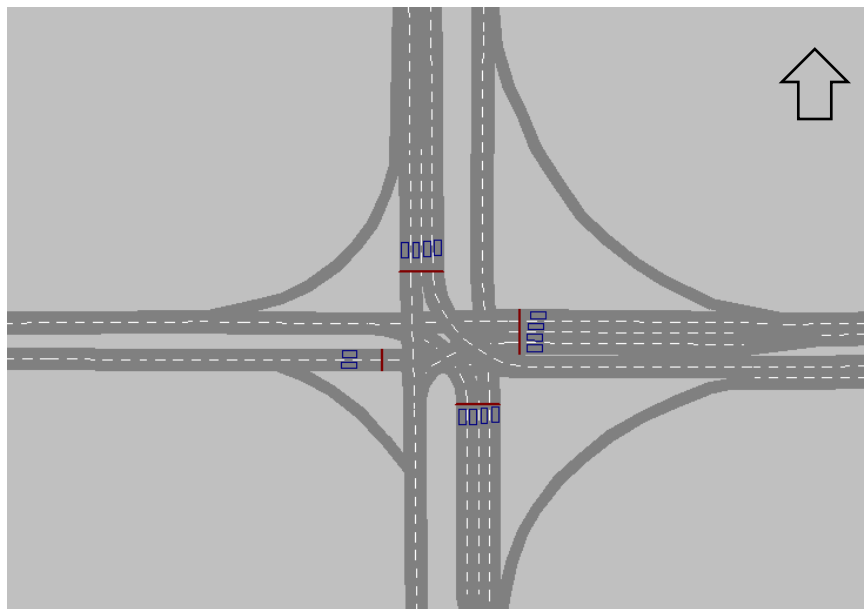
b) Eastbound Approach with Two Through Lanes

Figure 3-5. Site Characteristics of the Study Intersection Modeled in VISSIM

The conducted calibration of the VISSIM model was based on matching the saturation flow rates of the through movement, so that the capacity under blockage

condition from VISSIM matches the proposed model. Based on capacity outputs from VISSIM for various N (c_{VISSIM}), and the approach capacity from the proposed model under blockage condition (Equation (3-24)), the saturation flow rate for a single lane approach was obtained using the following equation:

$$s_T = c_{VISSIM} - \frac{3600}{C}(N+1)(1+\frac{V_R}{V_T}) + \frac{3600}{C}(N+1)(1-0.135p_r)\frac{C}{g(1-0.135p_r)} \quad (3\text{-}36)$$

where p_r is the proportion of right-turn traffic in the rightmost lane.

The same procedure was used for the case of multilane approach. Using the VISSIM results and the approach capacity from the proposed model under blockage condition, the saturation flow rate for a two-lane approach was obtained as follows:

$$s_T = c_{VISSIM} - \frac{3600}{C}(N+1)(1+\frac{V_R}{V_T}) + \frac{3600}{C}(N+1)(1-0.135p_r)\frac{C}{g(2-0.135p_r)} \quad (3\text{-}37)$$

Considering various right-turn volumes and short-lane section lengths, different scenarios were generated in VISSIM. The approach capacity was reported for the cases of single-lane and two-lane approach based on the following input data:

- Number of through lanes, $n = 1, 2$.

- Cycle length, $C = 110$ sec,

- Effective green time, $g = 32$ sec,

- Short-lane section length, $N = 3, 5, 7, 9$ and 11 vehicles,

- Proportion of right-turn traffic, $\dfrac{V_R}{V_T} = 0.1, 0.2, 0.3, 0.4, 0.5.$

A total of 250 runs (five runs for each of 50 scenarios) of simulation were done and then the average capacity of the five runs was reported. Using Equations (3-36) and (3-37), the through saturation flow rates were obtained for each scenario and then their average was reported. The average saturation flow rate for the case of single-lane approach was found to be about 2070 vph, while for the case of the two-lane approach was found to be 2135 vph. These inferred the through saturation headway of 1.74 and 1.69 seconds for the single lane and two-lane approaches, respectively. The through saturation flow rate obtained for both single-lane and two-lane approaches are higher than the typical value which is 1900 (vph). As Tian and Wu (2006) explained in their paper, with presence of right-turn lanes, larger gaps are created whenever a right-turn vehicle enters the right-turn lane. The larger gaps would allow the following vehicles to accelerate and catch up with the heading vehicles. This would result in an increased saturation flow rate.

The saturated flow rate for the shared-lane section was determined using a formula in the HCM presented in Equation (3-38):

$$s_N = f_{RT} s_T \tag{3-38}$$

$$f_{RT} = 1 - 0.135 p_r \tag{3-39}$$

The saturation flow rate for the right-turn movement was also obtained from VISSIM. A very large traffic volume was input into the VISSIM model to create a constant queue

in every cycle. Then, the difference between the time that the queue was formed and discharged in each cycle was calculated. Based on this calculation and the number of vehicles in the queue, the average discharge gap between vehicles was calculated. Based on a one-hour analysis period, the average discharge gap between right-turn vehicles was found to be 2.30 seconds. This implies the saturation flow rate of 1565 vph, which was obtained as follows:

$$s_R = \frac{3600}{2.30} = 1565 \text{vph} \tag{3-40}$$

The right-turn saturation flow rate was used in the approach capacity calculation under non-blockage condition (Equation (3-19)).

3.4.1. Validation of the Developed Blockage Probability Model

As discussed in Section 3.2, the probability of blockage was calculated by incorporating the influence of residual queues. Two methodologies, the HCM model and the DTMC model were used to estimate the expected residual queue at each cycle. Prior to evaluating the predictability of the blockage probability model, the results of these models were compared and validated against simulation. Then, the one with better estimates of the residual queue was applied in the blockage probability model.

Different scenarios considering various through volumes were generated and ran in VISSIM. The cycle length and the effective green time were set to 110 and 32 seconds, respectively. A total of 30 runs (five runs for each of six scenarios) were conducted and the residual queue in each cycle was reported through observation of the simulation models. The number of vehicles that arrived but were not served during each green

interval were counted and reported as the residual queue of each cycle. Then, the average of the observed residual queue was calculated and considered as the expected residual queue for each volume scenario. The simulation outputs as well as the results from both theoretical models are summarized in Table 3-1.

TABLE 3-1. Comparison of the Expected Residual Queue Estimates from HCM and DTMC Models and Simulation (in vehicles)

Through Volume (vphpl)	Simulation	HCM	DTMC
300	2	1	0
350	2	1	0
400	2	2	0
450	3	3	1
500	4	4	4
550	5	6	7

To visualize the goodness-of-fit of both theoretical models in estimating the expected residual queue, an illustration of their results was also provided in Figure 3-6. Each plot displays the VISSIM outputs of the simulation data versus the model outputs of the predicted data. Table 3-1 and Figure 3-6 clearly show that there is more consistency between the results from the HCM and simulation so the queue results from the HCM more closely match the results from simulation.

Even though the results of the HCM and the DTMC models did not significantly differ in the number of vehicles, they indirectly made a significant difference in estimates of the approach delay. The accurate estimation of the expected residual queue is necessary in estimating the probability of blockage which affects the approach capacity

and delay. Therefore, the HCM formula in this study was adopted to estimate the expected residual queue at each cycle.
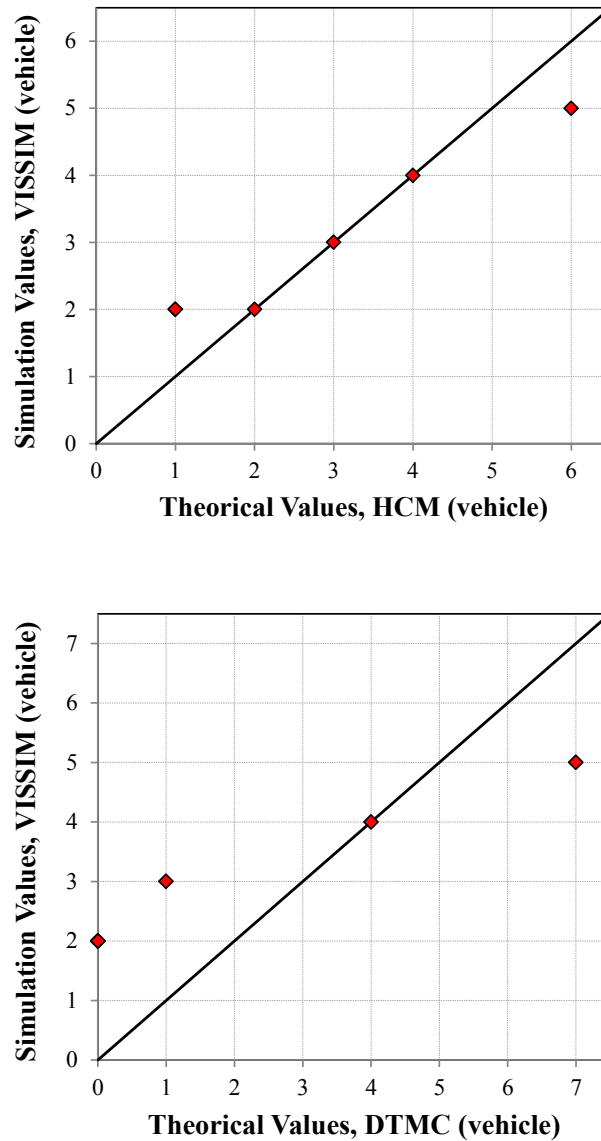
Figure 3-6. Comparison of Residual Queue Estimates from HCM and DTMC Methods vs. Simulation

To calculate the probability of blockage based on VISSIM outputs, one detector was located on the through lane where the right-turn channel begins and $(N+1)^{th}$ through vehicle can cause a blockage. The number of cycles when the detector was occupied by a

vehicle were counted and divided by the total number of cycles in the analysis period, which is one hour. In the other words, the proportion of cycles with a blockage to the total number of cycles in the analysis period was considered as the probability of blockage. However, in this case, the counted number of blockages included both acceptable and non-acceptable blockages (see Figure 3-2) because, through vehicles might overflow and block the channel entrance. Yet, all right-turn vehicles might have already passed through the channel before a blockage occurred. Therefore, when the detector is occupied, either of the blockages happened. Distinguishing between these two blockages in VISSIM was not feasible and required excessive number of simulation observations for different defined scenarios. The key input data into the VISSIM model was as follows:

- Cycle length, C=90 sec,

- Effective green time, g=27 sec,

- Short-lane section length, N=4 vehicles,

- Proportion of right-turn traffic, p_r =0.3.

Considering different volume-capacity ratios (v/c), different through volumes were put into the VISSIM model during the model validation. Seventy runs of simulation (10 runs for each of seven scenarios) were done. Then, the probability of blockage was calculated for each scenario and the average results of the 10 runs were reported. The warm-up time was set to 400 seconds and the simulation-recording period was set to 3600 seconds. The blockage probability results from the developed model were

calculated for each scenario. The probabilities of blockage obtained from VISSIM were compared to the sum of acceptable and unacceptable blockage probabilities obtained from the model. Figure 3-7 shows the validation of the developed blockage probability model.
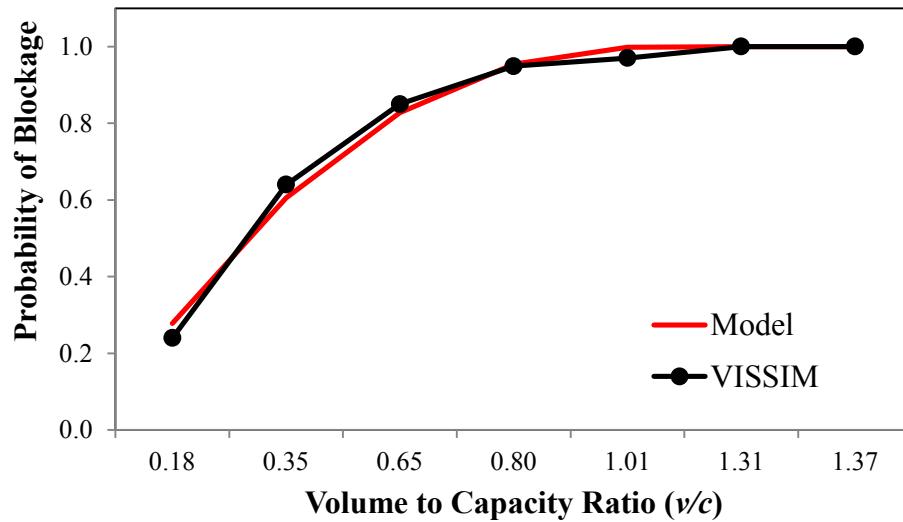
Figure 3-7. Validation of the Blockage Probability Model

Figure 3-7 shows that the results from the developed model almost match the obtained results from the simulation. The possibility of blockage increases with the increment of *v/c* ratio so in high ratios (e.g. more than 0.8), the blockage occurs almost every cycle. This happens because of the possible residual queues from the previous cycles, which result in the high probability of blockage in the next cycles.

3.4.2. Validation of the Traffic Distribution Model

As discussed in section 3.3.3, Tarko's method was adopted to estimate the traffic volume which uses the rightmost lane. An accurate estimate of traffic distribution between lanes is necessary because it significantly impacts the approach capacity and

delay. Therefore, in this section, the results of the proposed method are compared and validated against simulation. The outputs were obtained for different scenarios with the following key inputs:

- Cycle length, C=110 sec,

- Effective green time, g=32 sec,

- Through traffic volume, V_T =600,800, and 900 vph,

- Short-lane section length, N=3, 4, 5,..., 15 vehicles,

- Proportion of right-turn traffic, $\frac{V_R}{V_T}$ =0.1, 0.2.

The VISSIM model was run 10 times for each defined scenario so a total of 780 simulations were done. The outputs from VISSIM and the proposed model are plotted in Figure 3-8. The average error for each defined volume scenario was calculated as the weighed difference between the model and VISSIM and the results were summarized in Table 3-2.

It can be seen from Figure 3-8 and Table 3-2 that Tarko's model provided excellent estimates of the traffic volume in the rightmost lane with less than a five percent error.
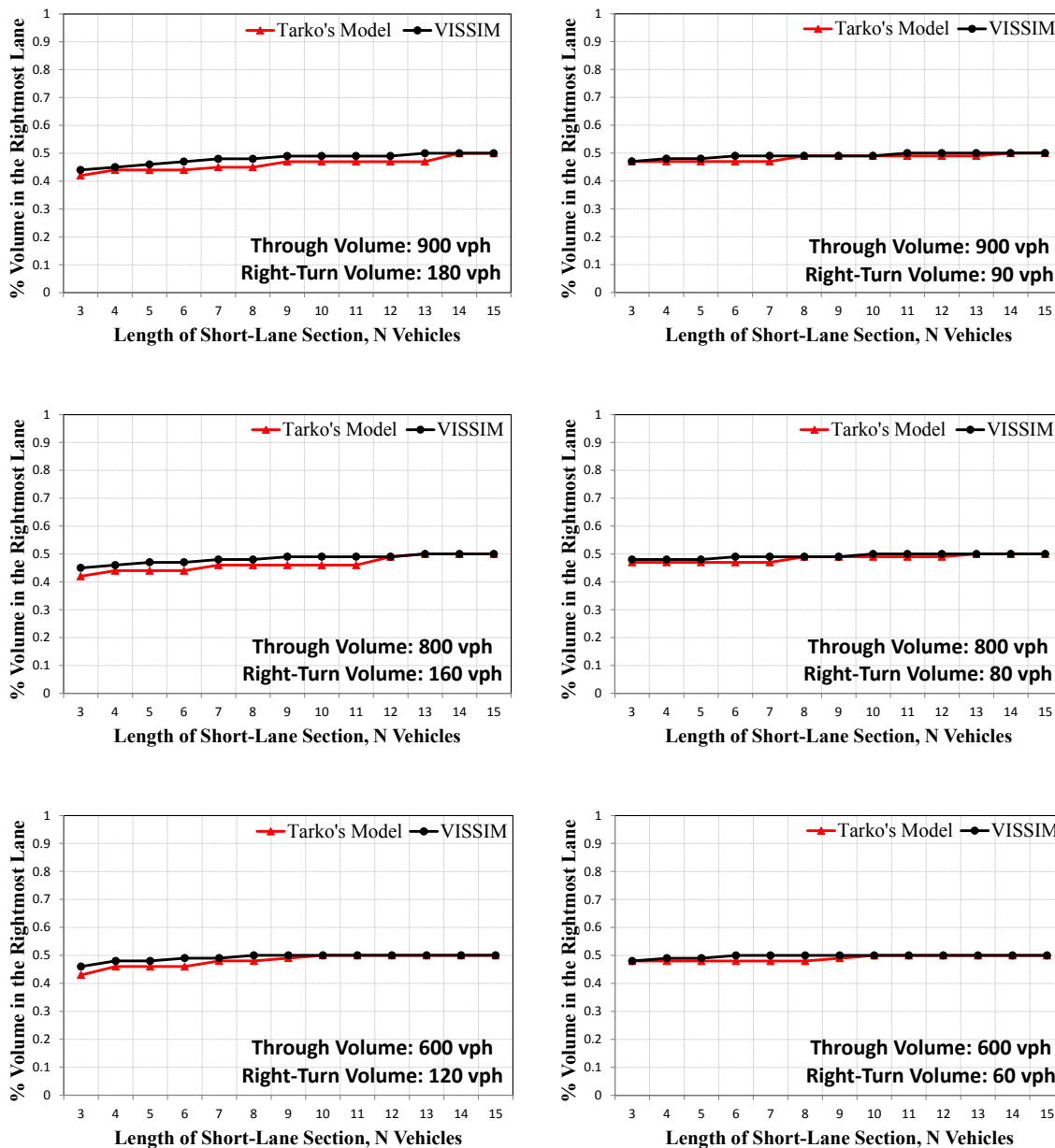
Figure 3-8. Proportion of Through Traffic Volume Using the Rightmost Lane, Estimates of Tarko's Model vs. VISSIM

TABLE 3-2. The Average Error between Tarko's Model and VISSIM in Estimating the Volume in the Rightmost Lane

Through Volume (vph)	$V_T=900$		$V_T=800$		$V_T=600$	
Right-turn Volume (vph)	$V_R=180$	$V_R=90$	$V_R=160$	$V_R=80$	$V_R=120$	$V_R=6$
Average Error	0.04	0.01	0.04	0.02	0.02	0.01

3.4.3. Validation of the Proposed Capacity Model under Blockage Condition

Since simulation software does not directly report the capacity, the capacity of a signalized approach should be measured based on the maximum flow rate that can be discharged under oversaturated conditions (Tian et al., 2007). The capacity results from VISSIM were obtained by increasing the demand until it reached its maximum. Under this condition, a blockage will occur in every cycle or 100 percent of the time (the probability of blockage equals 1.0). The maximum flow rate that can be discharged under this condition was considered and reported as the blockage capacity. In this research, obtaining the non-blockage capacity results from simulation was not be feasible, thus only the blockage capacity model was validated against simulation.

Different scenarios were generated by considering various right-turn volumes and short-lane section lengths. The key input data into the VISSIM model was as follows:

- Number of through lanes, $n = 1, 2$.

- Cycle length, $C=110$ sec,

- Effective green time, $g=32$ sec,

- Short-lane section length, $N=3, 5, 7, 9,$ and 11 vehicles,

- Proportion of right-turn traffic, $\dfrac{V_R}{V_T} =0.1, 0.2, 0.3, 0.4, 0.5$.

A total of 500 runs (10 runs for each of 50 scenarios) of simulation were done and the average of the reported discharged flows was considered as the blockage capacity for

each scenario. Figure 3-9 illustrates the validation of the proposed capacity model under blockage condition for the cases of single-lane and two-lane approach.
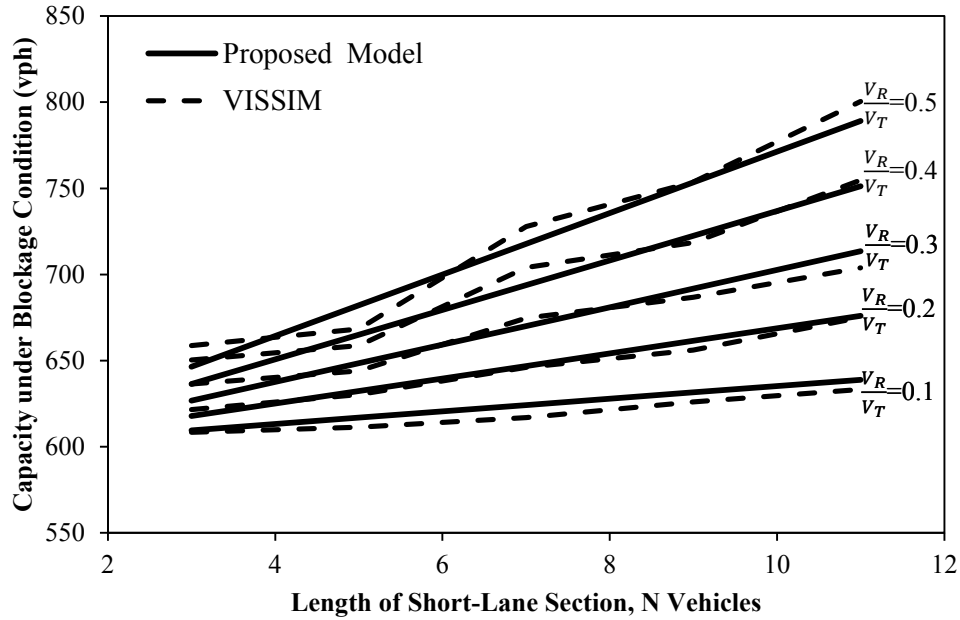
a) Capacity of a Single-lane Approach
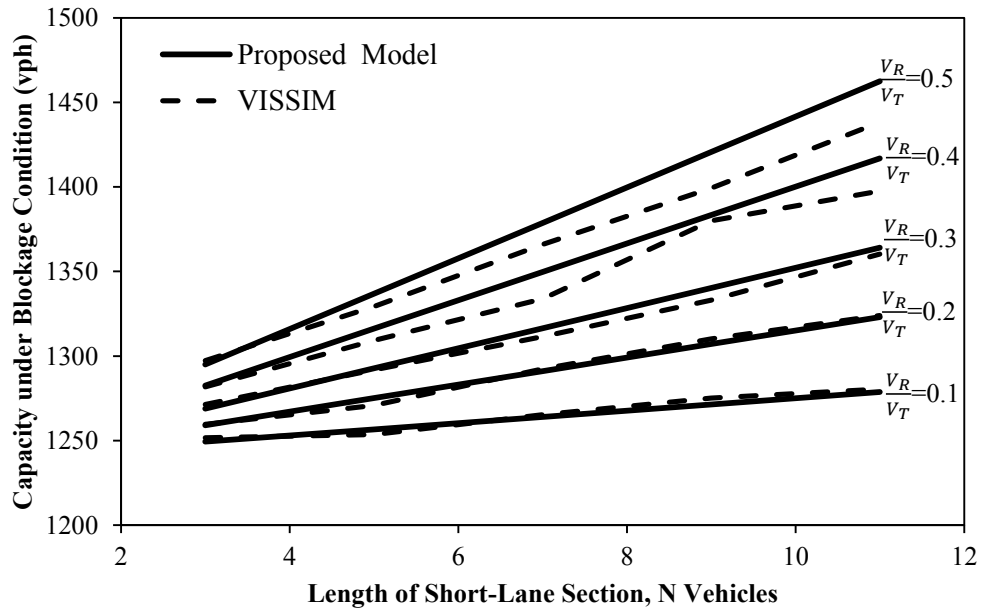
b) Capacity of a Two-lane Approach

Figure 3-9. Validation of the Proposed Capacity Model under Blockage Condition

As can be seen in Figure 3-9, the capacity results from the developed model closely match the obtained capacity results from the simulation model. It can be also seen that the approach capacity increases with the increment of N, especially when the proportion of right-turn traffic is higher.

3.5. RESULTS

To analyze the impact of a channelized right-turn lane on the capacity of a signalized approach, the approach capacity was estimated by considering different right-turn volumes and different lengths of the short-lane section. Figures 3-10 and 3-11 demonstrate the probability of blockage and the capacity results obtained based on the proposed models considering different lengths of the short-lane section and different proportions of right-turn traffic when the cycle length is 110 seconds and the effective green time is 32 seconds. The blockage probabilities were estimated by assuming the through volume of 450 vph. These results were generated for a single-lane approach.

As can be seen in Figure 3-10, there is a high probability of blockage when the length of short-lane section is short, especially when the proportion of right-turn traffic is relatively high. These blockage probabilities are only the probabilities of unacceptable blockage (Pattern 3 in Figure 3-2). From Figure 3-11, it is also evident that length of the short-lane section is a critical factor to the approach capacity especially for the cases of higher right-turn volumes. This is because the short-lane section length more significantly impacts the probability of blockage (see Figure 3-10). This means with a shorter short-

lane section, the percentage of right-turns has much more influence on the approach capacity. In summary, the percentage of right-turn traffic and the short-lane section length can significantly affect the approach capacity and consequently the approach delay.
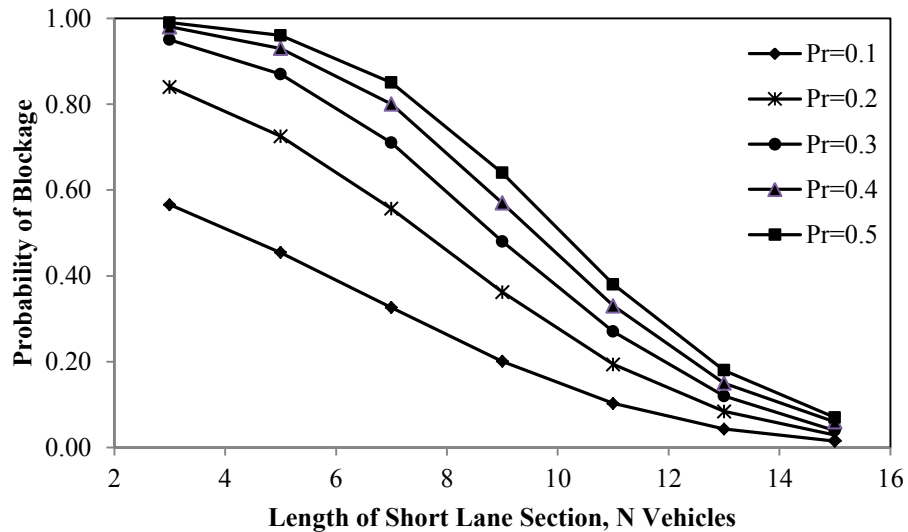
Figure 3-10. Impacts of *Pr* and *N* on the Probability of Blockage
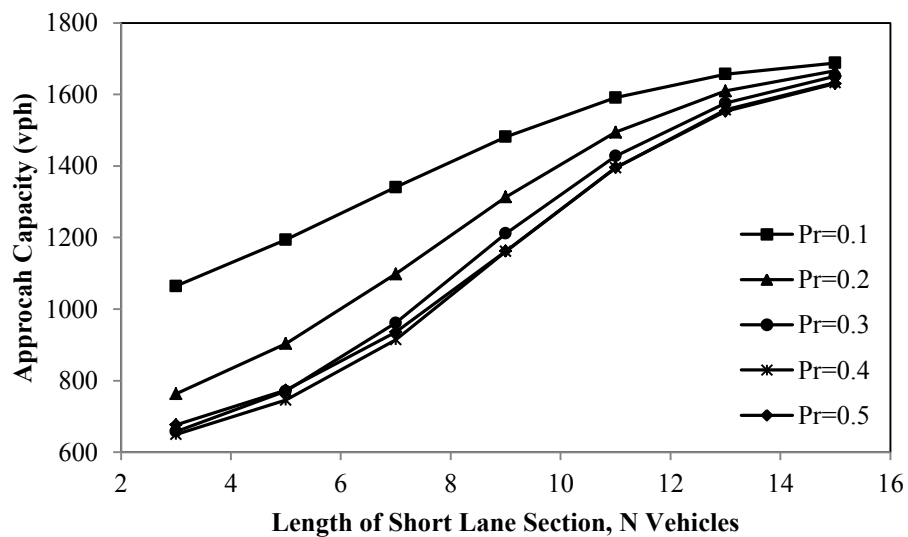
Figure 3-11. Impacts of *Pr* and *N* on the Single-lane Approach Capacity

3.5.1 Application of the Blockage Probability Model

With knowing the probability of blockage under different signal timing plans and arrival rates, lengths of the short-lane section can be determined. In this study, short-lane section lengths were determined to prevent the blockage in more than 95 percent of the cycles.

Table 3-3 shows the recommended lengths in feet and in the number of vehicles for different sets of through volumes, percentages of right-turn traffic, cycle lengths, and g/C ratios. The lengths were actually determined based on the five percent probability of unacceptable blockage (Pattern 3).

TABLE 3-3. Recommended Lengths of the Short-Lane Section in Number of Vehicles and Distance (in feet)

Cycle Length (second)	Through Volume (vphpl)	g/c Ratio=0.35			g/c Ratio=0.5		
		% Right-Turn =0.1	% Right-Turn =0.2	% Right-Turn =0.3	% Right-Turn =0.1	% Right-Turn =0.2	% Right-Turn =0.3
90	200	3(100)	4(125)	5(150)	2(75)	3(100)	4(125)
	300	6(200)	7(200)	8(225)	4(125)	5(150)	5(150)
	400	8(225)	9(250)	10	6(200)	7(200)	8(225)
120	200	4(125)	6(175)	6(200)	3(100)	4(125)	5(150)
	300	8(225)	9(250)	10(275)	6(200)	7(200)	8(225)
	400	11(300)	12(325)	13(350)	8(225)	10(275)	10(275)
150	200	6(175)	7(200)	8(225)	4(125)	5(150)	6(200)
	300	10(275)	11(300)	12(325)	8(225)	9(250)	10(275)
	400	14(375)	16(425)	16(425)	10(275)	12(325)	12(325)

The length of the short lane sections (in feet) were estimated based on the recommended method by Kikuchi et al. (1993) as follows:

$$L = N \times PCE \times L_P \qquad (3\text{-}41)$$

where,

- L_P is the average storage length of a passenger car (the value of 25 feet is assumed in the calculation), and

- *PCE* is the passenger car equivalent factor that is calculated using the following equation:

$$PCE = 1 + (E_B - 1)\, \text{Prob}_B + (E_T - 1)\, \text{Prob}_T \qquad (3\text{-}42)$$

where,

- Prob_B and Prob_T are the proportion of buses and trucks, respectively, and

- E_B and E_T are the *PCE*s of a bus and a truck with the recommended values of 2.1 and 2.9, respectively.

Assuming one and two percent as the percentages of buses and trucks, the recommended lengths of the short lane section were computed as shown in Table 3-3, values in parentheses. These values were rounded up to the nearest 25 feet.

The short-lane section lengths were found to be sensitive to the proportion of right-turn traffic and signal timing schemes. The recommended lengths would be useful for

evaluating the adequacy of the current lengths, identifying the options of extending the short-lane section length or changing the signal scheme to manage the blockage.

3.6. SUMMARY

This chapter proposed an analytical probabilistic model to estimate the approach capacity at signalized intersections with channelized right-turn lanes by considering the probability of blockage caused by through traffic. The blockage probability model was estimated by taking into account the possible residual queues from previous cycles. To validate the proposed models, a microscopic simulation model was built and calibrated based on matching the saturation flow rates of the through movement so that the approach capacities under blockage conditions from VISSIM matches those from the proposed model. The saturation flow rates for both single-lane and two-lane approaches were found to be greater than the typical value, which is 1900 vph. Such a discharge characteristic was explained by the car-following theory so that the through vehicles accelerate to catch up with the heading vehicles when larger gaps exist due to the presence of right-turn vehicles.

The proposed blockage probability model, the lane distribution model, and the capacity model under blockage condition were validated through simulation. Multiple scenarios of short-lane section lengths and proportions of right-turn traffic were generated to build the simulation model. The results showed a nearly perfect match between the developed models and simulation outputs.

It was found that the length of the short-lane section and the proportion of right-turn traffic affect the approach capacity, indicating that short sections significantly reduce the approach capacity especially when the right-turn volume was relatively high. This happens because there is a higher possibility of blockage with a shorter length of the short-lane section. The author recommends the incorporation of the proposed capacity model into the HCM, which does not provide any particular method of capacity estimation for signalized intersections with channelized right-turn lanes regarding the probability of blockage.

This study also developed the recommended lengths of the short-lane section for different signal plans with different cycle lengths and effective green times, and also different percentages of right-turn traffic. Three different queue patterns including non-blockage, acceptable blockage, and unacceptable blockage were identified and the probability of each pattern was calculated. Based on the given five percent threshold for the unacceptable blockage, lengths of the short lane section were obtained as the number of passenger cars. Then, the actual lengths were calculated considering the average vehicle length and the equivalent factor accounting for the traffic combination. The recommended lengths can be used either as a design procedure or as a criterion to evaluate the adequacy of the existing designs in terms of short-lane section lengths and signal timing schemes.

The proposed capacity model would be applicable to the actuated signals so that the expected actuated green time and cycle length should be computed and replaced by the effective green time and the cycle length. Even though the proposed models were built

assuming Poisson distribution for the vehicles' arrival pattern, the estimation can be modified for any other type of arrival distribution.

CHAPTER 4: MODELING APPROACH DELAY- PROBABILISTIC MODEL

4.1. INTRODUCTION

This chapter introduces a delay model for a signalized approach with a channelized right-turn lane considering the possibility of blockage. As stated earlier, HCM models cannot reflect the impact of right-turn blockage on the approach delay and, therefore, right-turn vehicles are treated as if they are not part of the approach. Therefore, when blockage occurs, HCM procedures would overestimate the capacity and underestimate the delay. Consequently, the current methodologies and software which model the delay based on the HCM would not accurately estimate the delay of the approaches with channelized right-turn lanes. Following the HCM procedure, the average control delay per vehicle for a given lane group was modeled by three components: uniform delay, random delay, and initial queue delay. In this study, no initial queue was assumed at the start of the analysis period so the third component, which accounts for delay due to an initial queue, took the value of zero. The proposed uniform delay was modeled based on queueing theory concepts, so the queue accumulation polygons (QAPs) were used as the main tool to estimate the approach uniform delay. The HCM procedure was followed to compute the random delay component using the lane group capacity estimated in Chapter 3.

The delay model derivation involved three major steps: (1) Calculating the approach uniform delay considering the blockage and non-blockage conditions; (2) Calculating the approach incremental delay due to the random fluctuation in the number of arrivals; (3) Calculating the control delay for the study lane group.

The proposed delay model enhances the conventional HCM models by considering different arrival and departure patterns under blockage and non-blockage conditions. Thus, it provides an improved delay estimate by considering the impact of short-lane section length, signal timing plans, and the distribution of traffic between lanes.

4.2. PROPOSED QAP UNIFORM DELAY

By assuming the uniform arrival distribution and using the average arrival rate in the queue accumulation polygons, it was not possible to reflect the impact of blockage on the approach delay estimates. In fact, the average number of vehicles that arrive during the red interval is a fixed value which could cause a blockage only when it is greater than the storage length of the short-lane section. For example, when the average volume is 400 vehicles per hour and the red interval is 78 seconds, almost nine vehicles arrive during the red interval. This creates a blockage for the conditions that the storage length of the short-section is less than nine vehicles. However, when the short-lane section can store more than nine vehicles e.g., 10 vehicles, still blockage could occur during some cycles. This is because of the fluctuation in vehicle arrival so that during some cycles, more than 10 vehicles may arrive resulting in a blockage. Therefore, to investigate the impact of

blockage on the approach delay, different scenarios were defined in this study based on the possible number of arrivals in red. The arrival scenarios in which the number of arrivals in red is less than the storage length of the short-lane section were considered as non-blockage conditions and the scenarios with more arrivals were considered as blockage conditions.

Two different QAPs were developed for the arrival scenarios in blockage and non-blockage conditions. Based on the corresponding QAPs and considering the probability of arrivals, the uniform delay was calculated for each arrival scenario. The number of possible scenarios depended on the maximum number of vehicles that could arrive during the red interval. The corresponding QAPs of the blockage and non-blockage conditions were developed and discussed in the following sections.

The approach delay was estimated by making similar assumptions to the capacity derivation process as follows:

e) First, a pre-timed signalized approach was assumed to include one through lane so the approach delay was estimated for this case. For the case of multiple through lanes, the delay was estimated for each lane group by making an adjustment on the lane utilization factor.

f) Through traffic demand was assumed to be high enough to cause blockage at some cycles at the start of the green interval.

g) The length of the right-turn lane was assumed to be long enough to avoid queue spillback to the beginning of the lane.

h) For simplicity, all the vehicles were assumed to be passenger cars.

4.2.1. Delay QAP under Non-Blockage Condition

As discussed in Chapter 3, for an approach with a channelized right-turn lane, a non-blockage condition happens when the number of through arrivals during the red interval is less than $(N+1)$ vehicles. In this situation, the number of through vehicles that arrive in red could be between zero and N vehicles ($X_{TH} = 0, 1, ..., N$). Therefore, the queue formed beyond the stop bar only consists of through vehicles that depart from the intersection after the onset of the green interval. In non-blockage conditions, right-turn vehicles do not experience any delay since they can proceed through the channel during the entire cycle time. The QAP shown in Figure 4-1 can be used to calculate the approach uniform delay for all the arrival scenarios under non-blockage conditions. The area under the queue curve illustrated in Figure 4-1 was calculated as the total approach uniform delay for each arrival scenario.

In Figure 4-1,

- X_{TH} is the number of through vehicles arriving during the red interval and form the queue to the condition that: $0 < X_{TH} < N+1$,

- V_{TH} is the equivalent through traffic (vehicles per hour) to the number of through arrivals in red, X_{TH}, and can be obtained as follows:

$$V_{TH} = \frac{X_{TH} \times 3600}{r} \tag{4-1}$$

where,

- r is the effective red time (sec),

- s_T is the discharge rate of the through movement (vph), and

- g_0 is the required green time (sec) for discharging the queued through vehicles and was obtained as follows:

$$g_0 = \frac{V_{TH} \times r}{s_T - V_{TH}}$$

(4-2)
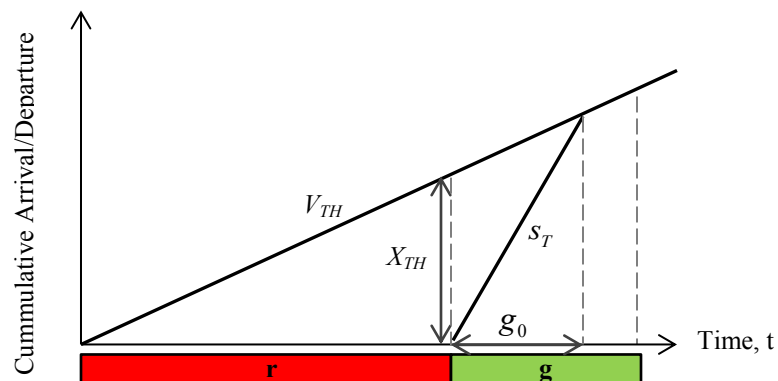
(a) Relationship between Arrivals, Departures, and Total Delay
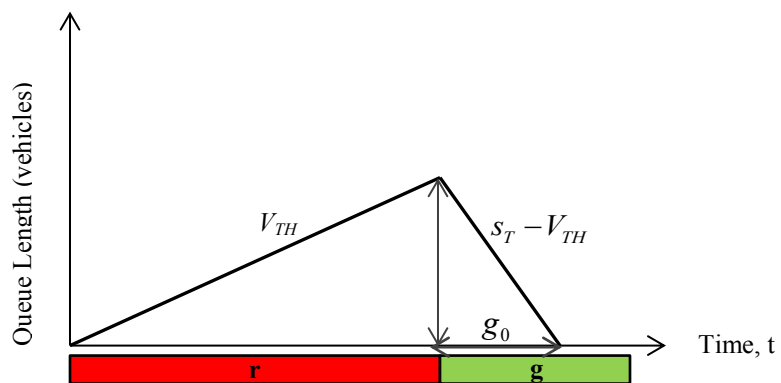
(b) Queue Accumulation Polygon (QAP)

Figure 4-1. An Illustration of the Approach Uniform Delay under Non-Blockage Conditions

Based on the illustration in Figure 4-1 and depending on the number of through arrivals in red, X_{TH}, the total approach uniform delay under non-blockage conditions for each arrival scenario can be calculated from the following equations:

$$D_{unblock}(i) = \frac{1}{2}[\frac{V_{TH}}{3600}(r+g_0)r] \quad \text{or} \tag{4-3}$$

$$D_{unblock}(i) = \frac{1}{2}[X_{TH}(r+g_0)] \qquad X_{TH} = 1,2,...,N \tag{4-4}$$

where, $D_{unblock}(i)$ is the total approach delay under non-blockage conditions for the ith arrival scenario; i can be 1,2,…,N corresponding to X_{TH}.

Then, Equation (4-5) was used to attain the average approach uniform delay for each scenario:

$$d_{unblock}(i) = \frac{D_{unblock}(i)}{\frac{V_i}{3600}C} \tag{4-5}$$

where,

- C is the cycle length (sec), and

- V_i is the approach arrival flow rate (vph) for the ith arrival scenario.

With knowing the through arrival flow rate and the proportion of through traffic, p_t, the approach arrival rate for each scenario can be obtained as follows:

$$V_i = \frac{1}{p_t} \times V_{TH} \tag{4-6}$$

4.2.2. Delay QAP under Blockage Condition

A blockage condition occurs by the arrival of $(N+1)^{th}$ through vehicle. In this situation, at least $(N+1)$ through vehicles arrive during the red interval and before onset of the green interval, which implies $X_{TH} = N+1, N+2, ...$ As discussed in the capacity derivation process, right-turn vehicles are able to get through the channel during the red interval before the arrival of $(N+1)^{th}$ through vehicle. Therefore, the first $(N+1)$ vehicles which form the queue, consist of only through vehicles. An illustration of the QAP under the blockage condition is shown in Figure 4-2 where the arrival rate for the first part of the red interval (t_1) is V_{TH} and for the remaining part of the red interval is V, which is the total approach arrival rate. This means that during t_1 right-turning vehicles do not experience any delay and they can get through the channelization. After the onset of the green interval, the first $N+1$ through vehicles in the queue start to discharge with the through saturation flow rate of s_T. Then, the vehicles beyond the channel throat start to discharge from the shared lane with the shared saturation flow rate of s_N. The QAP shown in Figure 4-2 can be used to calculate the approach uniform delay for all the arrival scenarios under blockage conditions. The area under the queue curve illustrated in Figure 4-2 was calculated as the total approach uniform delay for each arrival scenario.
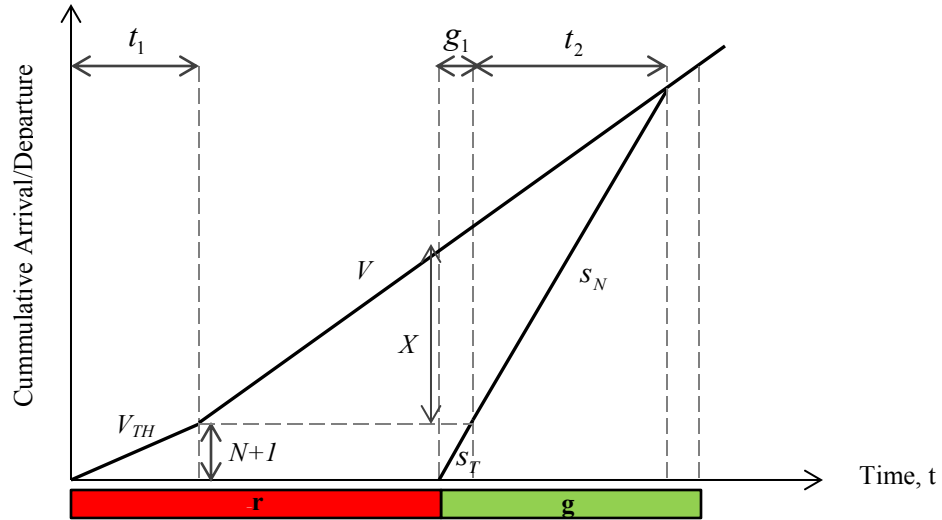
(c) Relationship between Arrivals, Departures, and Total Delay
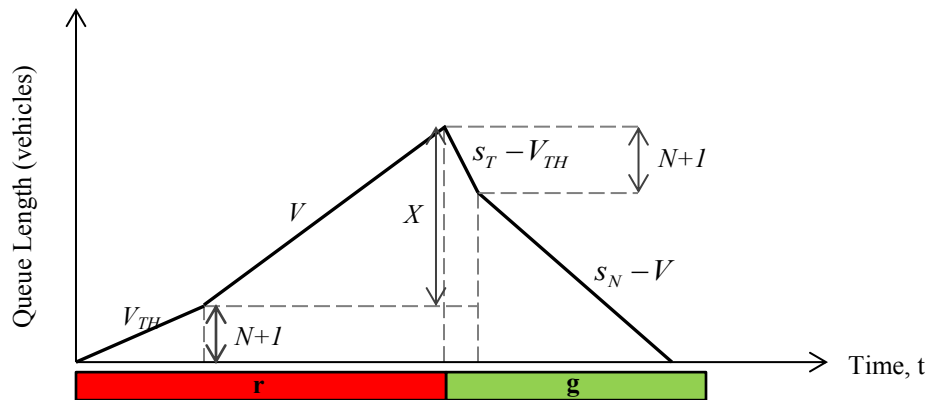
(d) Queue Accumulation Polygon (QAP)

Figure 4-2. An Illustration of the Approach Uniform Delay under Blockage Conditions

In Figure 4-2,

- X is the number of vehicles forming the queue beyond the channel throat, so in blockage conditions: $X_{TH} = X + (N+1)$ with $X \geq 0$,

- V is the approach arrival rate (vph) that can be obtained based on the proportion of through traffic as:

$$V = \frac{V_{TH}}{p_t} \tag{4-7}$$

- t_1 is the required time for arrival of the first $(N+1)$ through vehicles which was obtained based on the illustration in Figure 4-2 as follows:

$$t_1 = \frac{(N+1) \times r \times p_t^{-1}}{X + p_t^{-1} \times (N+1)} \tag{4-8}$$

- g_1 is the required green time for discharging first $(N+1)$ through vehicles in the queue with the through saturation flow rate of s_T and was obtained as follows:

$$g_1 = \frac{N+1}{s_T} \times 3600 + t_s \tag{4-9}$$

- t_2 is the remaining green time to discharge vehicles in the queue beyond the channel throat. Based on the illustration in Figure 4-2, it was obtained as follows:

$$t_2 = \begin{cases} \dfrac{V \times (r - t_1 + g_1)}{s_N - V} & t_2 \leq g - g_1 \\ g - g_1 & otherwise \end{cases} \tag{4-10}$$

In the blockage condition, different arrival scenarios were defined based on X. Using the illustration in Figure 4-2 and regarding X, the total approach uniform delay under blockage conditions for each arrival scenario can be calculated from Equation (4-11):

$$D_{block}(i) = \frac{1}{2}(N+1)t_1 + (N+1)(r - t_1) + \frac{1}{2}(N+1)g_1 + \frac{1}{2}[\frac{V}{3600}(r - t_1 + t_2 + g_1)^2 - s_N t_2^2] \tag{4-11}$$

Akin to non-blockage conditions, Equation (4-12) was used to calculate the average approach uniform delay for each arrival scenario:

$$d_{block}(i) = \frac{D_{block}(i)}{\frac{V_i}{3600}C}$$

(4-12)

4.2.3. Approach Uniform Delay

In previous sections, the approach uniform delay was calculated for different arrival scenarios under blockage and non-blockage conditions. The probability of each arrival scenario of X_{TH} is the probability that X_{TH} through vehicles arrive during the red interval. As stated in Chapter 3, for an isolated intersection, which is the concern of this research, it is reasonable to assume that the arrival pattern of vehicles follows Poisson distribution. Hence, the probability of ith arrival scenario would be obtained as:

$$P(i) = P(X_{TH} = i) = \frac{(\lambda_T)^{X_{TH}} e^{-\lambda_T}}{X_{TH}!} \qquad i = 1, 2, ... N+1, N+2, ... a_T^{max}$$

(4-13)

where,

- V_T is the average through arrival rate (vph),

- λ_T is the expected through vehicles that arrive in red, $\lambda_T = \frac{V_T * r}{3600}$, and

- a_T^{max} is the maximum number of through vehicles that could arrive in a cycle.

a_T^{max} was determined as the 99th percentile of the number of arrivals. This implies that a_T^{max} through vehicles arrives in more than 99 percent of cycles in an hour.

The approach uniform delay was obtained by applying the probabilities corresponding to arrival scenarios. The summation of all scenario delays was considered and reported as the total approach uniform delay:

$$d_1 = \sum_{i=1}^{N} d_{unblock}(i) \times P(i) + \sum_{i=N+1}^{a_T^{max}} d_{block}(i) \times P(i) \tag{4-14}$$

Using the above-mentioned process, an illustration of the approach uniform delay calculation is shown in Table 4-1.

TABLE 4-1. An Illustration of the Approach Uniform Delay Calculation Process

	No. of Through Vehicles Arrive in Red, $i = X_{TH}$	*Total Uniform Delay*	*Average Uniform Delay*	*Probable Average Uniform Delay*
Non-Blockage Condition	*1*	$D_{unblock}(1)$	$d_{unblock}(1)$	$d_{unblock}(1) \times P(X_{TH} = 1)$
	2	$D_{unblock}(2)$	$d_{unblock}(2)$	$d_{unblock}(2) \times P(X_{TH} = 2)$
	$\vdots$	$\vdots$	$\vdots$	$\vdots$
	N	$D_{unblock}(N)$	$d_{unblock}(N)$	$d_{unblock}(N) \times P(X_{TH} = N)$
Blockage Condition	*N+1*	$D_{block}(N+1)$	$d_{block}(N+1)$	$d_{block}(N+1) \times P(X_{TH} = N+1)$
	N+2	$D_{block}(N+2)$	$d_{block}(N+2)$	$d_{block}(N+2) \times P(X_{TH} = N+2)$
	$\vdots$	$\vdots$	$\vdots$	$\vdots$
	a_T^{max}	$D_{block}(a_T^{max})$	$d_{block}(a_T^{max})$	$d_{block}(a_T^{max}) \times P(X_{TH} = a_T^{max})$
		Approach Uniform Delay= d₁=		**SUM**

4.3. ESTIMATION OF THE RANDOM DELAY COMPONENT

The random delay component accounts for the delay due to the random fluctuation in number of arrivals and also the delay caused by partially oversaturated conditions which might happen during the analysis period. In this research, the HCM incremental delay formula was used to calculate the random delay component, which is derived using an assumption of no initial queue at the start of the analysis period:

$$d_2 = 900T\left[(X_L - 1) + \sqrt{(X_L - 1)^2 + \frac{8kIX_L}{c_L T}}\right]$$

(4-15)

In Equation (4-14):

- T is the length of the analysis period (hour),

- c_L is the lane group capacity (vph) which is calculated using the proposed procedure in Chapter 3,

- X_L is the volume to capacity ratio equal to $\frac{V_L}{c_L}$,

- k is a factor for the effect of controller type on delay. A value of 0.50 is recommended for pre-timed phases, and

- I is the upstream filtering adjustment factor, which accounts for the effect of an upstream signal on vehicle arrivals to the study lane group. The value of this factor is 1.0 for an isolated intersection.

The random delay term is valid for all values of X_L including undersaturated and oversaturated conditions. In Equation (4-15), the 15-minute analysis period is assumed, so *T=0.25*.

4.4. LANE GROUP CONTROL DELAY

The uniform delay and random delay values computed in the previous sections were added to estimate the control delay for the study lane group:

$$d = d_1 + d_2 \qquad (4\text{-}16)$$

A representative numerical example of the aforementioned procedure can be found in Appendix A.

4.5. DELAY OF A MULTILANE APPROACH

Similar to the approach capacity, in the case of multiple through lanes, one lane group can be associated with the rightmost lane where its control delay was estimated by applying the procedures provided in sections 4.2 to 4.4. The other lane group can be associated with the other through lanes. Equations (2-3) and (2-4) presented in Chapter 2 can be used to calculate the control delay of the other lane group consisting of through lanes. Following the HCM procedure, the average control delay for the intersection approach was calculated using Equation (4-17) in which each lane group delay is weighted by the lane group flow rate:

$$d_A = \frac{\sum\limits_{j=1}^{m} d_j V_j}{\sum\limits_{j=1}^{m} V_j} \qquad\qquad (4\text{-}17)$$

where, d_j is the control delay for lane group j (second per vehicle), V_j is the traffic volume in lane group j, and m is the number of lane groups in the study approach.

To obtain the traffic volume of the rightmost lane and the other lanes, the lane utilization or the traffic distribution between lanes needs to be determined. The through traffic departing form the rightmost through lane was estimated in section 3.3.3 of Chapter 3. Knowing the traffic volume of the rightmost lane, the procedure discussed in Section 4.2 was used to calculate the lane group control delay of the rightmost lane. Then, the HCM formula was applied to calculate the control delay of the other lane group, which consisted only of through lanes.

4.6. MODEL CALIBRATION AND VALIDATION

The data set used in Chapter 3 was also used in this chapter to calibrate and validate the proposed delay model. In Chapter 3, a VISSIM model was constructed and calibrated based on the data obtained from the simulation. In this chapter, the same calibrated model was used to validate the proposed delay model. The site characteristics of the study intersections are shown in Figure 4-3. The eastbound approaches with single and double through lanes and different lengths of the short-lane section were the study approaches with their signal timing plan shown in Table 4-2.
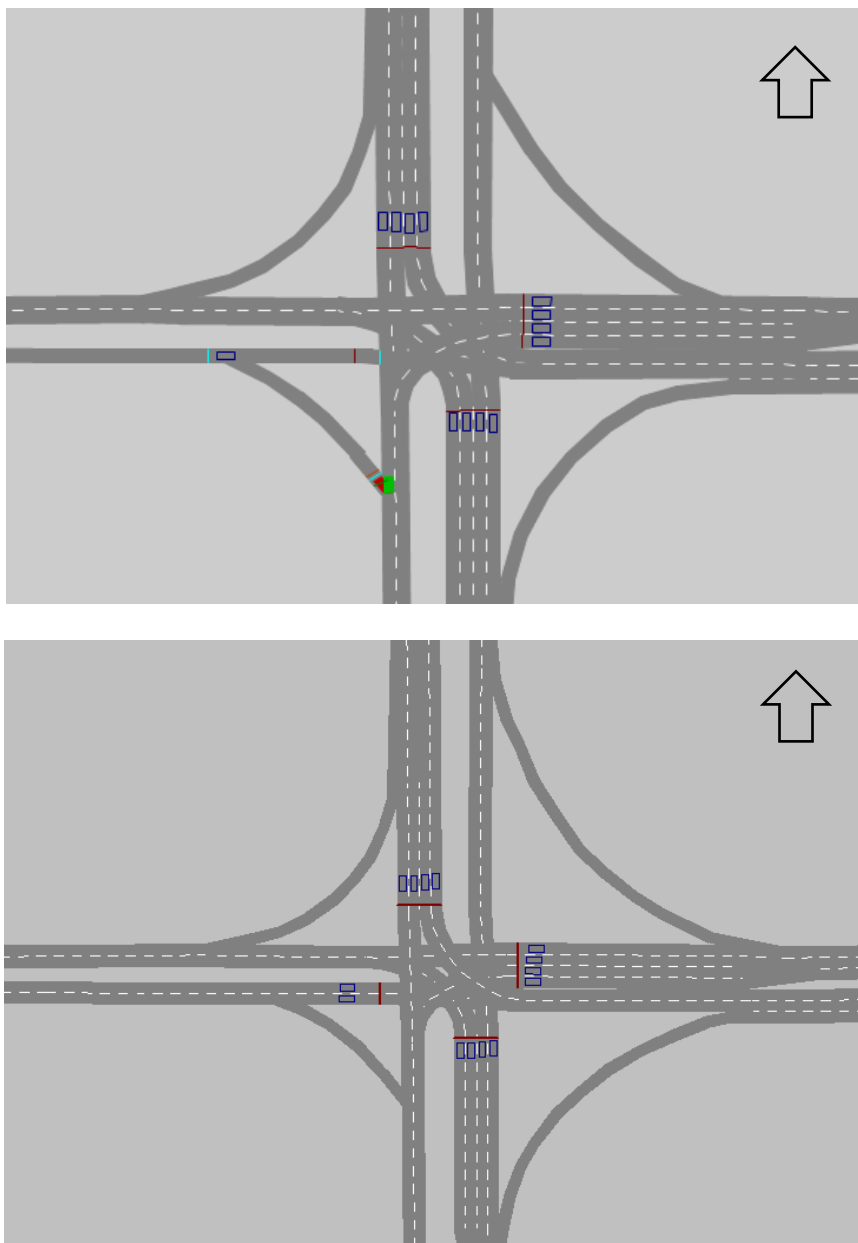
Figure 4-3. Site Characteristics of the Study Intersections Modeled in VISSIM

TABLE 4-2. Signal Timing Plan for the Study Approaches (sec)

Cycle Length, C	Phase Split	Vehicle Extension	Startup lost time, t_s	Yellow Interval	All Red	Effective Green Time, g
110	36	2	2	4	2	32

No field data was used for the validation process so the validation was done based only on the simulated data. There are two main reasons and advantages of using simulation. First, a significant and costly effort of data collection would be required for queue discharging and delay from the sites with various geometric conditions and signal timing plans. Second, various scenarios with different geometric and traffic conditions can only be created in a simulated environment. Due to the stochastic nature of simulation software, multiple runs of simulations are required for each scenario to avoid significant variation in results.

4.6.1. Validation of the Proposed Delay Model against VISSIM

Single-lane Approach

In VISSIM, the average delay is determined as the time difference between the actual travel time and the free-flow travel time along a user defined segment. The study segment is defined as a node so the travel time is measured between upstream and downstream boundaries of the defined node. Since VISSIM does not directly report the average approach delay and the delays are reported for individual movements, the HCM formula presented in Equation (4-16) was used to calculate the average delay of the study lane group. Different scenarios were generated by considering various through volumes, different percentage of right-turn traffic, and different lengths of the short-lane section. A total of 156 scenarios were created in VISSIM with the following key input data:

- Cycle length, C=110 sec,

- Effective green time, g=32 sec,

- Through traffic volume, V_T =200, 300, 400, 430 vph,

- Percentage of right-turn traffic, p_r =0.1, 0.2, 0.3,

- Short-lane section length, N=3, 4, …, 15 vehicles.

Due to the stochastic nature of simulation, the VISSIM model was run 10 times for each defined scenario so a total of 1,560 runs of simulation were done. Based on the reported through and right-turn movements' delays and following Equation (4-16), the average approach delay was calculated and considered as simulation output. VISSIM delay outputs are plotted in Figures 4-4 through 4-6. The estimated average approach delays were calculated using the procedure proposed in Sections 4.2 through 4.4 and are presented in these figures as well. The saturation flow rates of the through and right-turn movements that are required to estimate the approach delay were determined as discussed in Chapter 3, Section 3.4.

It can be seen in Figures 4-4, 4-5, and 4-6 that the approach delay from both the proposed and simulation models decreases as the length of the short-lane section increases. This implies the proposed model has the capability of reflecting the delay increase due to the right-turn channel blockage, which is not addressed in the HCM or any other references. The decreasing trend is more obvious for the scenarios of higher through and right-turn traffic volumes. This happens because there would be a higher possibility of blockage when more through vehicles arrive. Also, with more right-turn volume, more right-turn vehicles might experience a blockage and get trapped between the through vehicles queueing beyond the stop bar.

As can be seen in the figures, the delay seems to be underestimated by the proposed model especially when the length of the short-lane section is shorter. This could happen due to the different delay estimation processes utilized by the model and simulation. The simulation reports the delay based on the time difference between the actual travel time and the free-flow travel time along a study segment. Thus, it would take into account any delay due to the acceleration and deceleration that vehicles may experience when making frequent stops. However, the proposed theoretical model does not account for the delay resulting from frequent stops and other drivers' behavior. When there is a large traffic volume and higher subsequent possibility of blockage, vehicles might experience more frequent stop and go traffic and correspondingly longer delays. Nevertheless, overall, there is a good agreement between the proposed model and the simulation results.

To see the effectiveness of the proposed model in modeling the approach delay, the relative error which shows how the model outputs differ from the simulation outputs was calculated for each individual scenario using Equation (4-18).

$$\text{error} = \frac{\left|d_{Model}(N) - d_{VISSIM}(N)\right|}{d_{Model}(N)} \qquad N = 3, 4, \ldots, 15 \qquad \text{(4-18)}$$

Then, the mean error (ME) was calculated for each volume scenario illustrated in Figures 4-4 through 4-6 using Equation (4-19):

$$ME = \frac{1}{n} \sum_{N=3}^{15} \frac{\left|d_{Model}(N) - d_{VISSIM}(N)\right|}{d_{Model}(N)} \qquad \text{(4-19)}$$

where,

- N is the length of the short-lane section and varies from three to 15 vehicles,

- $D_{Model}(N)$ is the estimated approach delay when the length of short-lane section is

  N,

- $D_{VISSIM}(N)$ is the actual approach delay obtained from VISSIM when the length

  of short-lane section is *N*, and

- *n* is the number of short-lane lengths for which the approach delay is estimated

  (*n= (15-3) +1=13*),. The percent error and ME values for the defined volume

  scenarios are shown in Tables 4-3.

It can be seen from Table 4-3 that the average difference between the outputs from simulation and the proposed model is insignificant, so ME is less than five percent most of the time. This implies that the proposed model provides accurate estimates of the approach delay and reflects the blockage impact with approximately 95 percent of confidence level.

Figure 4-4. Single-lane Approach Delay Comparison, Model vs. VISSIM with 10% Right-Turns

Figure 4-5. Single-lane Approach Delay Comparison, Model vs. VISSIM with 20% Right-Turns
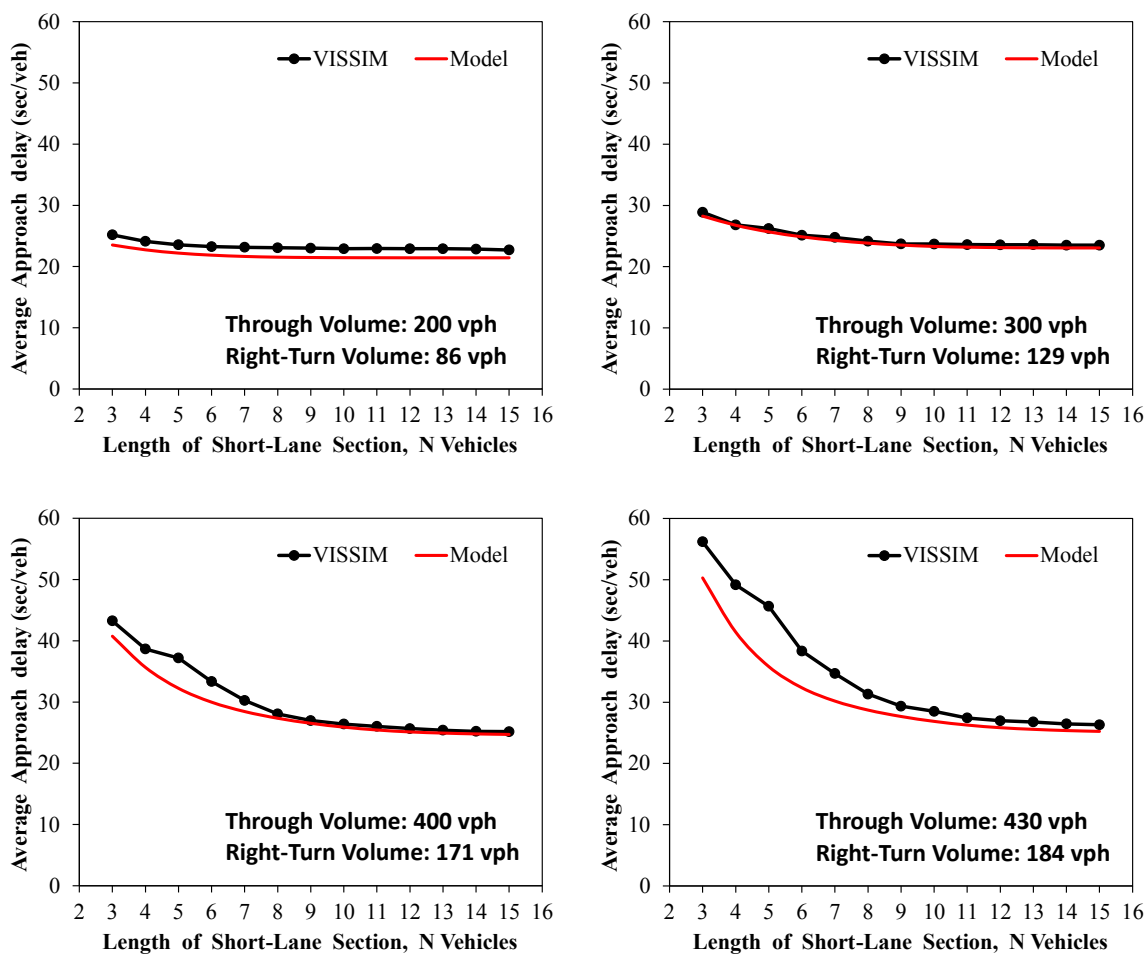
Figure 4-6. Single-lane Approach Delay Comparison, Model vs. VISSIM with 30% Right-Turns

TABLE 4-3. The Calculated Error between the Single-lane Approach Delay Estimates from the Proposed Delay Model and Simulation

N	$V_T=200$			$V_T=300$			$V_T=400$			$V_T=430$		
	$V_R=22$	$V_R=50$	$V_R=86$	$V_R=33$	$V_R=75$	$V_R=129$	$V_R=45$	$V_R=100$	$V_R=171$	$V_R=48$	$V_R=108$	$V_R=184$
3	0.06	0.03	0.07	0.03	0.04	0.02	0.02	0.04	0.06	0.03	0.08	0.12
4	0.06	0.04	0.06	0.03	0.01	0.00	0.02	0.05	0.08	0.04	0.06	0.19
5	0.07	0.04	0.06	0.02	0.00	0.02	0.01	0.07	0.15	0.04	0.11	0.27
6	0.07	0.04	0.06	0.02	0.00	0.01	0.00	0.07	0.11	0.04	0.08	0.19
7	0.07	0.05	0.07	0.01	0.01	0.02	0.00	0.05	0.06	0.03	0.07	0.15
8	0.06	0.05	0.07	0.00	0.02	0.01	0.01	0.03	0.03	0.04	0.06	0.09
9	0.06	0.06	0.07	0.01	0.03	0.01	0.01	0.03	0.02	0.05	0.06	0.06
10	0.06	0.06	0.07	0.01	0.04	0.02	0.02	0.03	0.02	0.06	0.06	0.06
11	0.06	0.06	0.07	0.01	0.04	0.02	0.03	0.04	0.02	0.07	0.06	0.04
12	0.06	0.06	0.07	0.02	0.04	0.02	0.03	0.04	0.02	0.07	0.06	0.04
13	0.06	0.06	0.07	0.02	0.04	0.02	0.03	0.04	0.02	0.07	0.06	0.05
14	0.06	0.06	0.07	0.02	0.04	0.02	0.03	0.04	0.02	0.07	0.06	0.04
15	0.06	0.04	0.06	0.02	0.04	0.02	0.04	0.04	0.02	0.07	0.06	0.04
ME	0.06	0.05	0.07	0.02	0.03	0.02	0.02	0.04	0.05	0.05	0.07	0.1

Two-lane Approach

The proposed delay model for the case of multilane approach was also validated against VISSIM by analyzing two through lanes. Similar to the single-lane approach, different scenarios were generated to build the VISSIM model by considering the following key input data:

- Number of through lanes, $n=2$,

- Cycle length, $C=110$ sec,

- Effective green time, $g=32$ sec,

- Through traffic volume, $V_T =600, 800, 900$ vph,

- Percentage of right-turn traffic, $p_r =0.1, 0.2$,

- Short-lane section length, $N=3, 4, \ldots 15$ vehicles.

A total of 104 scenarios were run in VISSIM and each scenario was run 10 times. As a result, a total of 1,040 simulations were conducted. The VISSIM delay outputs are plotted in Figures 4-7 and 4-8. The estimated average approach delays calculated using the procedure proposed in section 4.5, are presented in these figures as well. The delay outputs from the proposed model were computed with respect to lane distribution results obtained from VISSIM. This was done to create more consistency between model and simulation delay outputs, although an excellent match was found between Tarko's model and simulation outputs for the lane utilization.
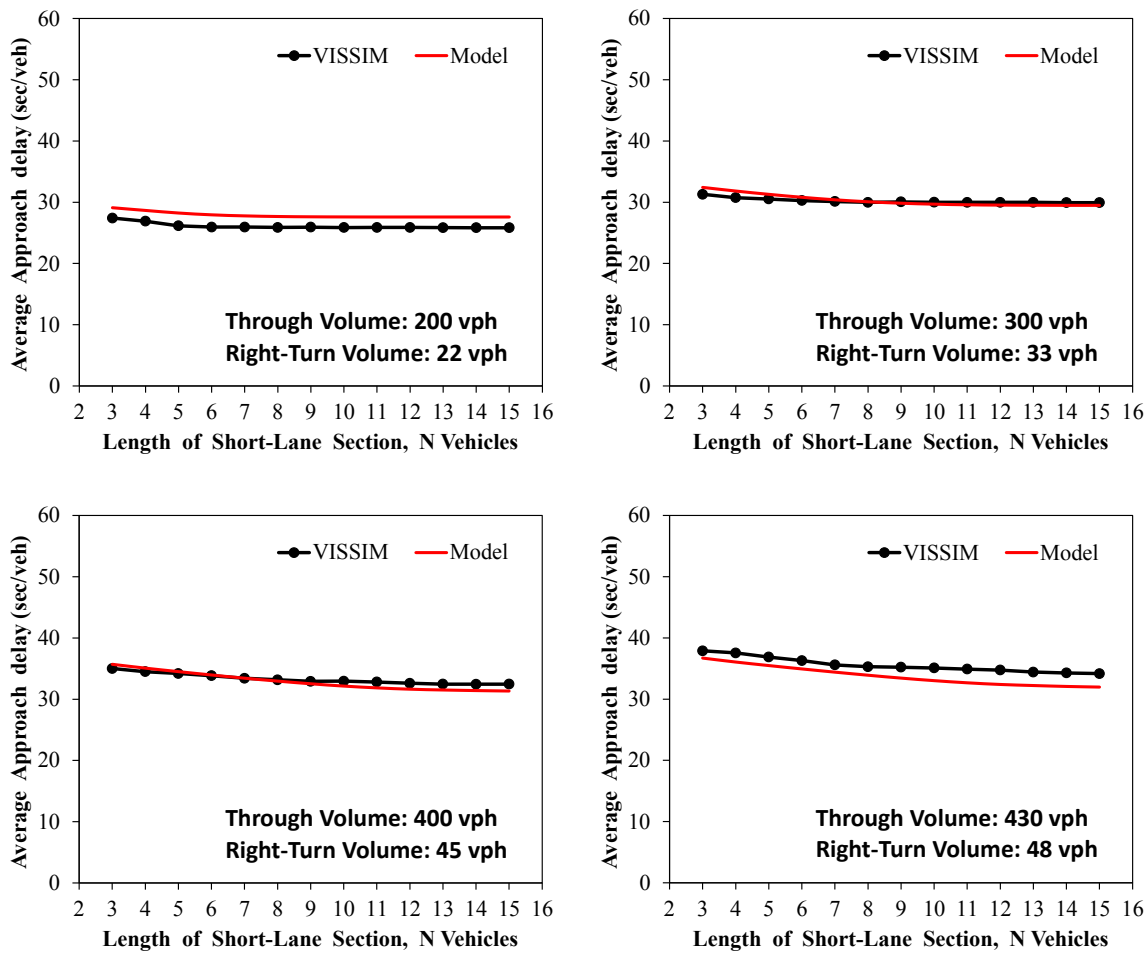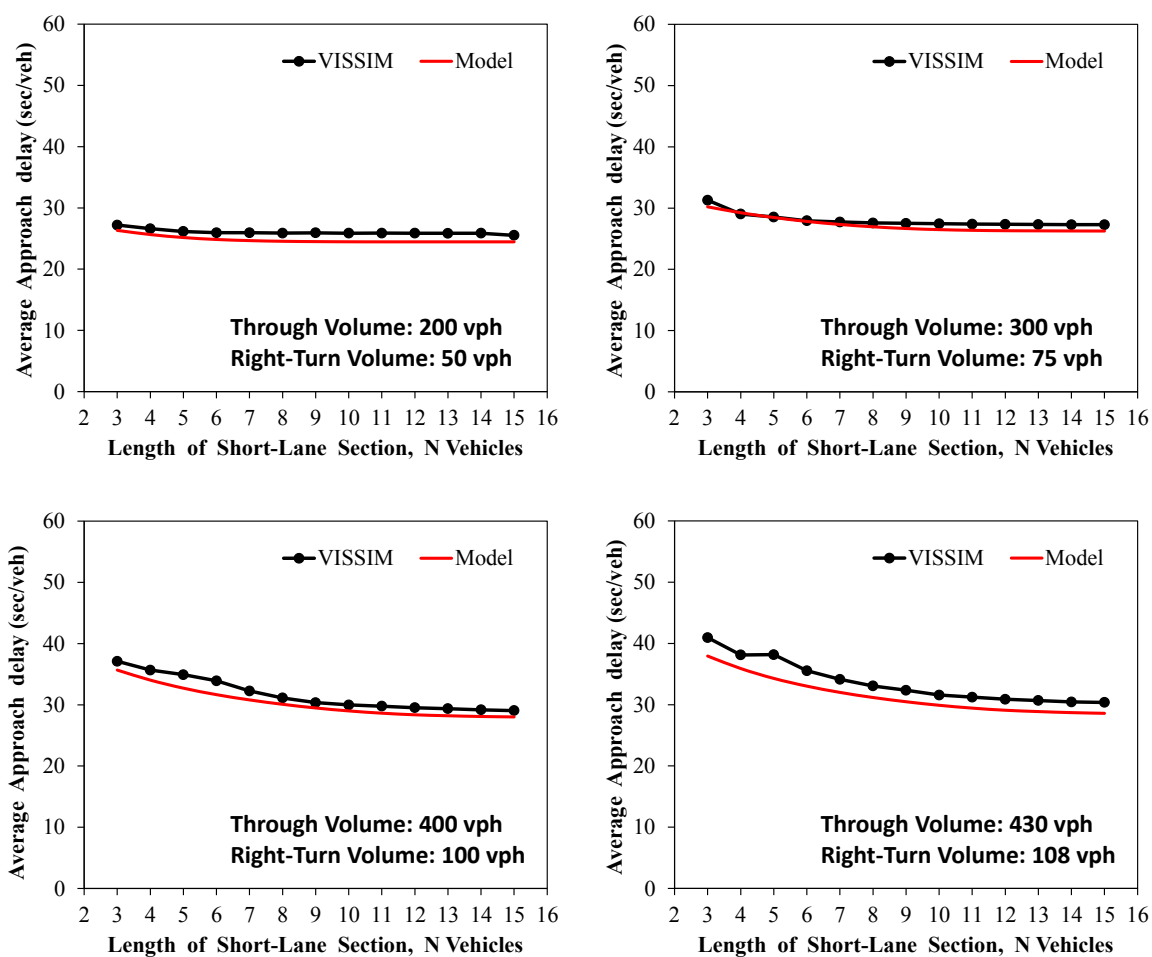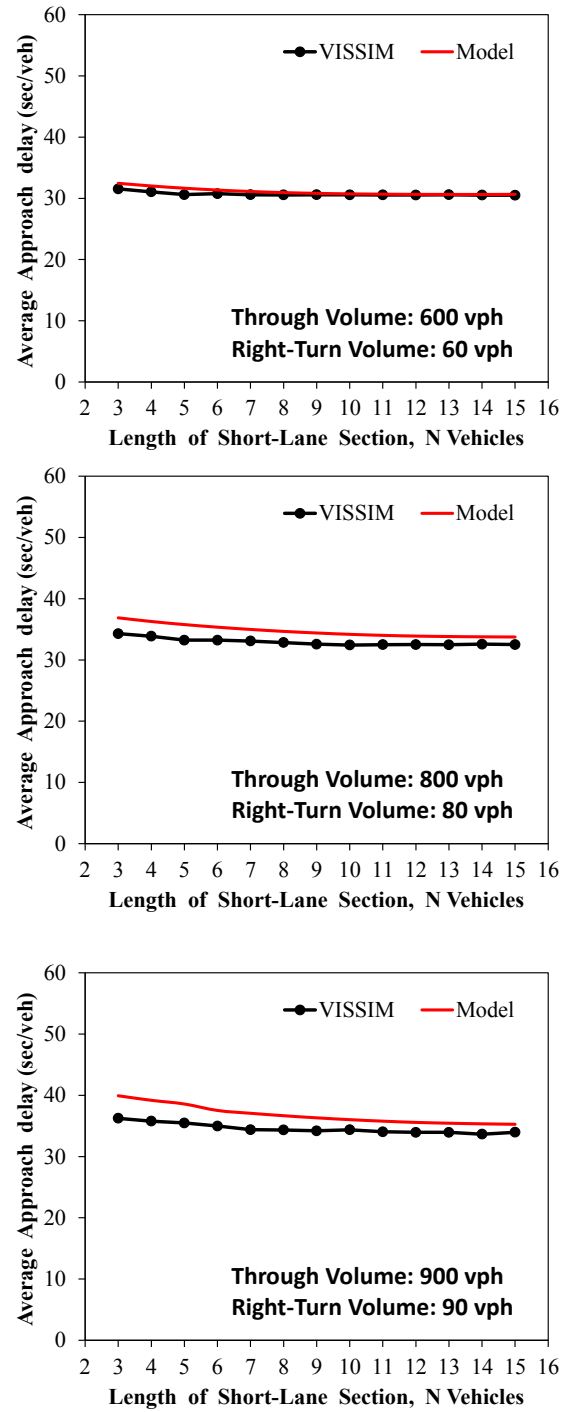
Figure 4-7. Two-lane Approach Delay Comparison, Model vs. VISSIM with 10% Right-Turns
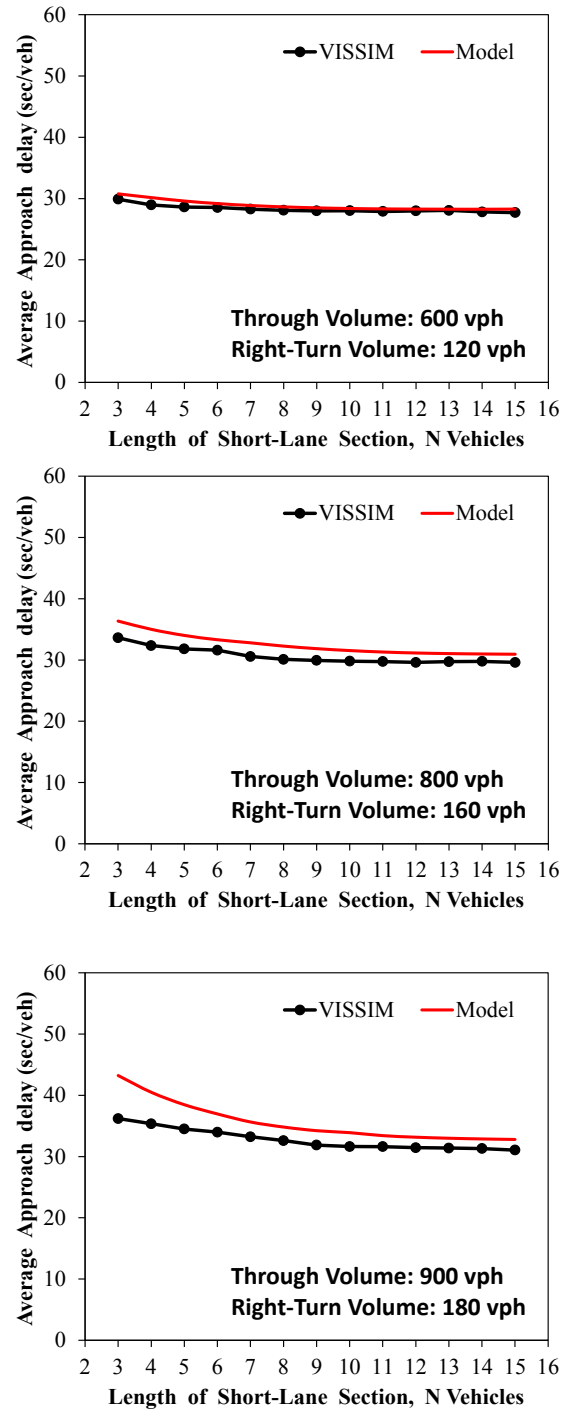
Figure 4-8. Two-lane Approach Delay Comparison, Model vs. VISSIM with 20% Right-Turns

Similar to the single-lane approach, a decreasing trend was found in the approach delay while length of the short-lane section increased. The proposed model for the multilane approach also has the capability of reflecting the delay increase due to the right-turn channel blockage, which is not addressed in the HCM or any other references. The decreasing trend is more obvious for the scenarios of higher through and right-turn traffic volumes.

Unlike the case of single-lane approach, as can be seen in Figures 4-7 and 4-8, the delay seems to be overestimated by the proposed model, especially when the length of the short-lane section is shorter and there is higher traffic volume. One possible reason that might have contributed to such a difference is the lane change behavior, which is not addressed in the proposed model. With the presence of right-turn lanes, there is a possibility of blockage at the rightmost lane that makes right-turn vehicles wait for the blockage to disappear. This may create a slow traffic stream in the rightmost lane at some cycles and discourage vehicles from using the rightmost lane. Although the impact of blockage has been addressed in the lane distribution model to estimate the average volume in the rightmost lane, some vehicles might decide to change their lane just when they are departing from the intersection. The immediate lane change behavior in the case of blockage may reduce the total delay experience by drivers. Therefore, VISSIM produced lower delays. The potential lane change behavior was not accounted for in the theoretical proposed model and it was not easily feasible to incorporate it into the proposed model. Particularly, when there is high traffic volume and subsequently higher possibility of blockage, vehicles might change their lane more frequently to suffer less

delay. Nevertheless, in general, there is a reasonable agreement between the proposed model and the simulation outputs.

The calculated error and the average error for each volume scenario illustrated in Figures 4-7 and 4-8 are summarized in Table 4-4.

As can be seen from Table 4-4, there is no significant difference between the outputs from simulation and the proposed model. This implies that the proposed model provides accurate estimates of the approach delay and reflects the blockage impact at an approximate 95% percent confidence level.

TABLE 4-4. The Calculated Error between the Two-lane Approach Delay Estimates from the Proposed Delay Model and Simulation

N	$V_T=600$		$V_T=800$		$V_T=900$	
	$V_R=60$	$V_R=120$	$V_R=80$	$V_R=160$	$V_R=90$	$V_R=180$
3	0.03	0.03	0.07	0.07	0.09	0.16
4	0.03	0.04	0.07	0.08	0.09	0.13
5	0.03	0.03	0.07	0.07	0.08	0.10
6	0.02	0.02	0.06	0.05	0.07	0.08
7	0.02	0.02	0.05	0.07	0.07	0.07
8	0.01	0.02	0.05	0.07	0.06	0.06
9	0.01	0.02	0.05	0.06	0.06	0.07
10	0.00	0.01	0.05	0.05	0.05	0.07
11	0.00	0.01	0.04	0.05	0.05	0.05
12	0.00	0.01	0.04	0.05	0.05	0.05
13	0.00	0.01	0.04	0.04	0.04	0.05
14	0.00	0.02	0.04	0.04	0.05	0.05
15	0.01	0.02	0.04	0.04	0.04	0.05
ME	**0.01**	**0.02**	**0.05**	**0.06**	**0.06**	**0.08**

4.7. SUMMARY

This chapter proposed a delay model for pre-timed signalized approaches with channelized right-turn lanes considering the impact of blockage. The QAPs were used to develop the approach uniform delay and the HCM procedure was followed to compute the incremental delay caused by the random fluctuation of vehicle arrivals. No initial queue was assumed at the start of the analysis period so the third component of delay, which accounts for delay due to an initial queue, was assumed to be zero.

To investigate the impact of blockage on the uniform delay, different scenarios were defined based on the possible number of arrivals in red. The arrival scenarios with the arrivals less than the storage length of the short-lane section were considered as non-blockage conditions and the scenarios with more arrivals were considered as blockage conditions. Therefore, two different QAPs were developed based on the arrivals in blockage and non-blockage conditions. According to the HCM and considering the probability distribution of arrivals, the area under the polygons was calculated as the uniform delay for each arrival scenario. The arrival pattern of vehicles was assumed to follow the Poisson process.

A wide range of traffic scenarios were created in VISSIM to validate the proposed delay model for the cases of single-lane and two-lane approaches. Overall, good matches were found between the proposed models and simulation outputs, proving that the proposed models could provide accurate estimates of the approach delay and reflect the blockage impact with 95 percent confidence level. In case of a single-lane approach, the proposed model underestimated the delay approach. The difference between the proposed

model and simulation could be related to the difference in the delay estimation procedure. Simulation models can take into account any delay due to the acceleration and deceleration that vehicles might experience when making frequent stop and go travel. The theoretical proposed model cannot account for this affect or drivers' behavior. When there is high traffic volume and subsequently higher possibility of blockage, vehicles might experience more frequent stop and go resulting in longer delay. This is why there is a bigger difference between the proposed model and simulation outputs when traffic volumes are higher.

Unlike a single-lane approach, the proposed delay model overestimated the approach delay for the case of a two-lane approach. Drivers' lane changing behavior could have contributed to this difference. At some points, when there is slow traffic stream due to a blockage, some drivers may decide to change their lane and use the other lane when departing from the intersection. This may reduce the delay that they experience. Although the volume distribution between the lanes was estimated by considering the impact of blockage, modeling the immediate lane changes is not easily feasible.

In summary, the proposed delay model enhances the conventional HCM models by considering different arrival and departure patterns under blockage and non-blockage conditions. Thus, it provides improved delay estimates by considering the impact of short-lane section length, signal timing plans, and the probability distribution of traffic arrivals.

Using the proposed model, the following findings were discovered:

- The proposed model has the capability of reflecting the delay increase due to the right-turn channel blockage. The approach delay decreases as the length of short-lane section increases. The decreasing trend is not addressed in the HCM, which indicates the limitation of the current HCM procedure.

- Through and right-turn volumes significantly influence the approach delay estimates. A sharper decreasing trend was found in delay for the cases of higher through and right-turn traffic volumes. This happens because there would be a higher possibility of blockage when more through vehicles arrive. Also, with more right-turn volume, more right-turn vehicles might experience a blockage and get trapped between the through vehicles queueing beyond the stop bar.

CHAPTER 5: SUMMARY AND CONCLUSIONS

5.1. MAJOR FINDINGS

This research was conducted to develop probabilistic capacity and delay models for signalized intersections with channelized right-turn lanes considering the probability of blockage caused by through vehicles. Compared with the widely used HCM procedures for estimating the capacity and delay, the proposed models reflect the impact of blockage on the capacity and delay while the HCM dos not. Using the standard methods for estimating the capacity and delay without taking into account the impact of blockage would lead to the overestimation of the approach capacity and underestimation of the approach delay.

The capacity development process involved estimation of capacity under blockage and non-blockage conditions and applying the corresponding probabilities. The blockage probability model was developed with respect to the residual queues from previous cycles. To obtain the residual queues, two methodologies were applied and compared with each other: (1) Discrete-time Markov Chain (DTMC), and (2) HCM formula. Both methodologies were validated through VISSIM and it turned out that the HCM formula is more consistent with the VISSIM outputs. Since then, the HCM formula was used to calculate the probability of blockage and consequently, in the capacity estimation model. In addition, VISSIM was also used to validate both the blockage probability model and

the proposed capacity model under blockage conditions. The results showed a nearly perfect match between the developed models and VISSIM outputs.

In addition, this study developed the recommended lengths of the short-lane section in terms of number of vehicles by using the blockage probability model and defining a five percent threshold as the probability of blockage. Lengths of the short-lane section were obtained and reported by considering different cycle lengths, effective green times, and different proportions of right-turn traffic. Afterwards, the actual distances in feet were reported considering the average vehicle length and the equivalent factor accounting for the traffic combination.

The concept of QAPs was used to estimate the approach uniform delay and the HCM procedure was followed to compute the random delay component. Two different QAPs were developed regarding arrival scenarios in blockage and non-blockage conditions. To validate the proposed delay model, a wide range of traffic scenarios were modeled in VISSIM considering different short-lane section-lengths and different through and right-turn traffic volumes. Validation showed there was a good agreement between the proposed model and simulation outputs, indicating the proposed model can provide accurate estimates of approach delay and reflect the blockage impact very well.

Based on the analysis conducted in this research, the major findings and conclusions are summarized as follows:

- Short-lane section length and proportion of right-turn traffic influence the approach capacity so that short sections significantly reduce the approach capacity, especially when the right-turn volume is relatively high.

- The recommended short-lane section lengths can be used either as a design procedure to evaluate the adequacy of the existing designs in terms of geometry and signal timing schemes, to identify the options of extending the short-lane section length, or change timing plans to manage the blockage.

- The proposed delay model could provide accurate estimates of the approach delay and reflect the blockage impact at an approximate 95 percent confidence level.

- The impact of blockage to the right-turn channel was reflected in the proposed delay model. Using the proposed model, the approach delay decreases as the length of the short-lane section increases. Nevertheless, this decreasing trend is not addressed in the HCM, indicating the limitation of the current HCM procedure.

- Through and right-turn volumes significantly influence the approach delay. A sharp decreasing trend in delay was found against the short-lane section lengths for the cases of high through and right-turn volumes.

- The proposed delay model for the case of single-lane approach underestimated the approach delay. Their difference was explained as the difference in delay estimation process. The simulation models report the delay

by taking into account the deceleration or acceleration that vehicles may experience due to the frequent stop and go. The theoretical proposed model did not account for this effect or driver behavior. Therefore, it would be reasonable to get lower estimates of delay by the proposed model.

- The proposed delay model for the case of two-lane approach overestimated the approach delay. The difference might be related to the lane changing behavior of drivers. The presence of right-turn vehicles and possibly a slow traffic stream due to a blockage would discourage drivers to use the rightmost lane. Therefore, some through vehicles may suddenly change their lane when discharging the intersection to reduce their delay. Although the impact of blockage was addressed in the lane distribution model to determine the volume in the rightmost lane, these sudden lane changes are not easily feasible to be modeled.

- The proposed capacity and delay models were recommended to be incorporated into the HCM, which does not provide separate methods of capacity and delay estimation for intersections with channelized right-turn lanes, particularly accounting for the impact of blockage.

5.2. RECOMMENDATIONS FOR FUTURE RESEARCH

Several research areas are identified for future studies:

- The proposed models can be further expanded by addressing the case of right-turn spillback into the through lane. In this study, the proposed capacity and delay models were developed with the assumption that no right-turn spillback occurs. This assumption is true most of the time, especially when the right-turn volume is low and the right-turn channel is long enough to avoid any spillback. However, in the case of heavy right-turn traffic, since right-turn vehicles are not free and need to yield to the upcoming vehicles, their queue might spillback and causes a blockage to the through vehicles. The probability of right-turn spillback needs to be estimated by considering right-turn arrival and capacity when they yield to the upcoming vehicles and wait for an acceptable gap to merge into the traffic. In addition, the queue spillback possibility strongly depends on the length and radius of the right-turn channel, which identifies how many vehicles can be stored.

- The delay that right-turn vehicles experience where they yield to vehicles on the side street was not included in the delay estimation process. Similarly, to be consistent with the model results, the simulation outputs also were reported in a way to exclude that part of delay. In other words, right-turn vehicles were treated as if they do not contribute to the approach delay after entering the channel. If it is desired to estimate the delay that vehicles experience when they complete their movement, the right-turn delay due to their yield needs to be estimated and added to the proposed approach delay.

- In this study, for simplicity, all the vehicles were assumed to be passenger cars. This is not what happens in a real-world condition. In real cases, there might be heavy vehicles which turn at lower speeds than passenger cars and also a blockage will occur with fewer numbers of vehicles. To find a general agreement between the results from proposed models and real world situations, using filed data from intersections with different traffic composition and possibly different drivers' behavior is recommended. Calibration of the simulation models considering different traffic characteristics not only are a better representative of a real-world situation, but also will help customizing models for areas with different characteristics.

- The proposed delay models were limited to a case of an isolated signalized intersection. Thus, the arrival pattern of vehicles was assumed to be random following the Poisson process. Other types of vehicle arrival distributions considering the platoon arrival are recommended for investigation in future research.

REFERENCES

Highway Capacity Manual (HCM). (2010). Washington D.C.: Transportation Reserach Board o the National Academies.

(2011). *Policy on Geometric Design of Highways and Streets (6th Edition).* Washington D.C.: American Association of State Highway Transportation Officials (AASHTO).

Akcelik, R. (1998). *A Queue Model for HCM 2000.* Vermont South, Australia: Technical Note. ARRB Transport Research Ltd.

Akcelik, R. (2011). *Time-Dependent Expressions for Delay, Stop Rate and Queue Length at Traffic Signals.* Vermont South, Australia: Internal Report: Australian Road Reserach Board.

Fambro, D. B. and Rouphail, N. M. (1997). Generalized Delay Model for Signalized Intersections and Arterial Streets. *Transportation Research Record: Journal of the Transportation Research Board, 1572*, 112-121.

Gao, H. (2011). *Delay Models at signalized Intersections Considering Short-Right-Turn Lanes and Right-turn on Red.* University of Nevada, Reno.

Kikuchi S. and Kronprasert, N. (2008). Determining the Length of the Right-Turn Lane at a Signalized Intersection. *Transportation Research Record: Journal of the Transportation Research Board, 2060*, 19-28.

Kikuchi, S. and Kronprasert, N. (2010). Determining Lengths of Left-Turn Lanes at Signalized Intersections under Different Left-Turn signal Schemes. *Transportation Research Record, Journal of Transportation Research Board, 2195*, 70-81.

Kikuchi, S., Chakroborty, P., and Vukadinovic, K. (1993). Lengths of Left-turn Lanes at Signalized Intersections. *Transportation Research Record, Journal of the Transportation Research Board, 1385*, 162-171.

Kikuchi, S., Kii, M. and Chakroborty, P. . (2004). Lengths of Double or Dual Left-Turn Lanes. *Transportation Research Record, Journal of Transportation Research Board, 1881*, 72-78.

Kikuchi, S., Kronprasert, N. and Kii, M. . (2007). Lengths of Turn Lanes on Intersection Approaches: Three-Branch Fork Lanes-Left-Turn, Through, and Right-Turn Lanes. *Transportation Research Record, Journal of Transportation Research Board, 2023*, 92-101.

Kimber R. M. and Hollis, E. M. (1979). *Traffic queues and delay at road junctions.* Wokingham, Berkshire, United Kingdom: Transport And Road Research Laboratory.

Koonce, P., Rodegerdts, L., Lee, K., Quayle, S., Beaird, S., Braud, C., Bonneson, J., Tarnoff, P., and Urbanik, T. (2008). *Signal Timing Manual.* Washington, DC: U.S. Department of Transportation, Federal Highway Administration (FHWA).

Macfarlane, G. S., Mitsuru, S. and Schultz, G. G. (2011). Delay underestimation at free right-turn channelized intersections. *Procedia - Social and Behavioral Sciences, 16*(6th International Symposium on Highway Capacity and Quality of Service), 560-567.

Newell, G. F. (1965). Approximation Methods for Queues with Application to the Fixed-Cycle traffic Light. *Society for Industrial and Applied Mathematics (siam), 7*(2), 223-240.

Olszewski, P. S. (1990). Modeling of Queue Probability Distribution at Traffic Signals. *International Symposium on Transportation and Traffic Theory* (pp. 569-588). Yokohama, Japan: Elsevior Science Publishing Co., Inc.

Qi, Y., Azimi, M. and Guo, L. (2007). Determination of Storage Lengths of Left-Turn Lanes at Signalized Intersections. *Transportation Research Record, Journal of Transportation Research Board, 2023*, 102-111.

Qsei-Asamoah A., Kulshrestha, A., Washburn, S. S. and Yin, Y. (2010). Impact of Left-Turn Spillover on Through Movement Discharge at Signalized Intersections. *Transportataion Research Board, Journal of Transportataion Research Record, 2173*, 80-88.

Reynolds W. L., Rouphail, N. M. and Zhou, X. (2011). Turn Pocket Blockage and Spillback Models: Applications to Signal Timing and Capacity Analysis. *Journal of Transportataion Record, Journal of Transportataion Research Board, 2259*, 112-122.

Roess, R. P., Prassas, E. S. and McShane, W. R. (2004). *Traffic engineering (3rd Edition).* Prentice Hall.

Tarko, A.P. (2007). Predicting Right Turns on Red. *Transportation Research Record: Journal of the Transportation Research Board*, Vol.1776, pp.138-142.

Tian, Z. and Wu, N. (2006). Probbaalistic Model for Signalized Intersection Capacity with a Short Right-Turn Lane. *Journal of Transportation Enginerring, 132*(3), 205-212.

Tian, Z., Kyte, M., Vandehey, M., Kittelson, W., and Robinson, B. (2007). Simulation Based Study on Traffic Operational Characteristics at All-Way Stop-controlled

Intersections. *Transportation Research Record, Journal of the Transportation Research Board, 1776*, 75-81.

Tian, Z., Urbanik, T., Engelbrecht, R. and Balke, K. (2002). Variations on capacity and delay estimates from microscopic simulation models. *Transportation Reserach Record: Journal of Transportation Research Board, 1802*, 23-31.

Wu, N. (2011). Modeling Blockage Probability and Capacity of Shared Lanes at Signalized Intersections. *Procedia - Social and Behavioral Sciences, 16*, 481-491.

Yin, K., Zhang, Y. and Wang, B. X. . (2012). Modeling Delay During Heavy Traffic for Signalized Intersections with Short Left-Trun Bays. *Transportation Research Record: Journal of the Transportation Research Board, 2257*, 103-110.

Zhang, Y. and Tong, J. (2008). Modeling Left-Turn Blockage and capacity at Signalized Intersection with Short Left-Turn Bay. *Transportation Research Record: Journal of Transportation Research Board, 2071*, 71-76.

APPENDIX A: NUMERICAL EXAMPLE

Notation:

a_T^{max} : Maximum number of through vehicles that could arrive in a cycle (veh)

a_R^{max} : Maximum number of right-turn vehicles that could arrive in a cycle (veh)

C : Cycle length (sec)

c_L : Capacity of lane group L (vph)

c_{block} : Approach capacity under blockage condition (vph)

$c_{non-block}$: Approach capacity under non blockage condition (vph)

$D_{unblock}(i)$: Total approach delay under non-blockage condition for i^{th} arrival scenario (sec)

$d_{unblock}(i)$: Average approach delay under non-blockage condition for i^{th} arrival scenario (sec/veh)

$D_{block}(i)$: Total approach delay under blockage condition for i^{th} arrival scenario (sec)

$d_{block}(i)$: Average approach delay under non-blockage condition for i^{th} arrival scenario (sec/veh)

d_1 : approach uniform delay (sec/veh)

d_2 : approach random delay (sec/veh)

d : approach control delay (sec/veh)

$d_{Model}(N)$: Estimated control delay from the proposed model when the length of short-lane section is N vehicles (sec/veh)

$D_{VISSIM}(N)$: Actual control delay obtained from VISSIM when the length of short-lane section is N vehicles (sec/veh)

$E(q) = Q_2$: The average residual queue which at each cycle (veh)

f_{RT} : Right-turn adjustment factor

g : Effective green time (sec)

g_1 : The required green time for discharging $N+1$ vehicles (sec)

g_0 : The required green time for discharging the queued through vehicles (sec)

I : Upstream filtering factor for platoon arrivals which is equal to 1.0 for isolated intersections

i : Arrival scenario in which I number of through vehicles arrive in red, it could be i=1,2,…, N

k_B : The adjustment factor related to early arrivals

MPE : mean percentage error

N : Length of the short-lane section (veh)

P_{block} : Probability of blockage

p_r : Proportion of right-turn traffic

p_t : Proportion of through traffic

$P(i)$: The probability of ith arrival scenario or arrival of I through vehicles in red

r : Effective red time (sec)

s_T : Saturation flow rate of the through movement (vph) which is obtained from the simulation to be 2000 (vph)

s_R : Saturation flow rate of the right-turn movement (vph) which is obtained from the simulation to be 1565 (vph)

s_N : Saturation flow rate of the shared lane (vph)

s_L : Saturation flow rate of lane group L (vph)

T : Length of the analysis period (h)

t_s : Startup lost time which is assumed to be 2 sec

t_1 : Required time for arrival of $N+1$ vehicles (sec)

t_2 : Remaining green time to discharge the vehicles in the queue beyond the channel throat (sec)

V_T : The average through volume (vph)

V_{TH} : The equivalent through traffic to the number of through arrivals in red, X_{TH}, (vph)

V_i : Approach arrival flow rate corresponding to the ith scenario (vph)

V_R : The average right-turn volume (vph)

V : Approach arrival rate associate with V_{TH} and the proportion of through traffic (vph)

X_T : Number of through vehicles that arrive in red (veh)

X_R : Number of right-turn vehicles that arrive in red (veh)

X_{TH} : Number of through vehicles that arrive during the red phase and form the queue beyond the stop bar (veh)

X_L : Volume to capacity ratio of lane group L

X : Number of vehicles which form the queue beyond the channel throat in blockage condition (veh)

λ_T : The expected through vehicles that arrive in red (veh)

λ_R : The expected right-turn vehicles that arrive in red (veh)

λ_T^C : The expected through vehicles that arrive in a cycle (veh)

λ_R^C : The expected right-turn vehicles that arrive in a cycle (veh)

The proposed capacity and delay model explained in Chapters 3 and 4 are used to determine the capacity and delay of a pre-timed signalized approach with one through lane and a channelized right-turn lane as depicted in Figure A-1. The calculation is done by assuming the following data:

$V_T = 400\text{vph}$ Or $P_t = 80\%$
$V_R = 100\text{vph}$ Or $P_r = 20\%$
$C = 110\sec$
$g = 32\sec$
$s_T = 2070\text{vph}$
$s_R = 1565\text{vph}$
$N = 3, 4, ..., 15\text{veh}$
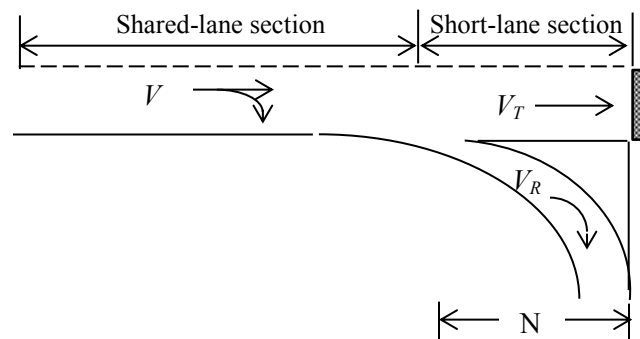
Figure A-1 A Signalized Single-lane Approach with Channelized Right-turn Lane

First, the probability of unacceptable blockage is calculated using the proposed probability model in Chapter 3, and then the approach capacity is determined by calculating the blockage and non-blockage capacities and applying their respected probabilities. After that, using the capacity results, the random delay component, d_2, which is dependent on the approach capacity, is obtained for each short-lane section scenario. Finally, the uniform delay component is determined based on the proposed delay model in Chapter 4 and the approach delay is calculated and reported as the

summation of uniform and random delays. In the calculation process, no initial queue is assumed at the start of the analysis period. Therefore, the third delay component which is due to an initial queue gets the value of zero. In the following, the calculation steps are presented in details.

Step 1- Calculate the through movement capacity, volume to capacity ratio, and the adjustment factor related to early arrivals:

$$s_N = (1 - 0.135 p_r) s_T = (1 - 0.135 \times 0.2) \times 2070 = 2014 \text{vph}$$

$$c_L = \frac{g}{C} s_N = \frac{g}{C} (1 - 0.135 p_r) s_T = \frac{32}{110} \times 2014 = 585.89 \text{vph}$$

$$X_L = \frac{V_L}{c_L} = \frac{400}{585.89} = 0.68$$

$$k_B = 0.12 I \left(\frac{s_L g}{3600} \right)^{0.7} = 0.12 \times 1 \times \left(\frac{2070 \times 32}{3600} \right)^{0.7} = 0.92$$

Step 2- Calculate the expected value of the residual queue following the HCM method and assuming 15 minutes analysis period, $T = 0.25\text{h}$:

$$E(q) = Q_2 = 0.25 c_L T \left[(X_L - 1) + \sqrt{(X_L - 1)^2 + \frac{8 k_B X_L}{c_L T} + \frac{16 k_B Q_{bL}}{(c_L T)^2}} \right]$$

$$= 0.25 \times 585.89 \times 0.25 \left[(0.68 - 1) + \sqrt{(0.68 - 1)^2 + \frac{8 \times 0.92 \times 0.68}{585.89 \times 0.25}} \right] \simeq$$

* Using the Markov Chain Model, the expected residual queue is obtained zero vehicle.

Step 3- Calculate the parameters required for determining the probability of blockage.

a_T^{max} and a_R^{max} which are the maximum number of through and right-turn vehicles arrive in a cycle, respectively are determined from the following equations:

$$P(through \quad arrivals \quad in \quad red = X_T) = \sum_{X_T=0}^{a_T^{max}} \frac{(\lambda_T^C)^{X_T} e^{-\lambda_T^C}}{X_T!} = 0.95$$

$$P(right-turn \quad arrivals \quad in \quad red = X_R) = \sum_{X_R=0}^{a_R^{max}} \frac{(\lambda_R^C)^{X_R} e^{-\lambda_R^C}}{X_R!} = 0.95$$

where, $\lambda_T^C = \dfrac{V_T * C}{3600}$ and $\lambda_R^C = \dfrac{V_R * C}{3600}$.

The above mentioned parameters which are used to calculate the probability of blockage are obtained as outputs of a macro in Excel. The results are summarized in Table A-1.

TABLE A-1 Input and Output Required Data to Calculate the Probability of Blockage

Input		Output		Max # of arrivals in a cycle
V_T	400	$\lambda_T = \dfrac{V_T * r}{3600} = \dfrac{400 * 78}{3600} =$	8.67	$a_{TH}^{max} = 18$
V_R	100	$\lambda_R = \dfrac{V_R * r}{3600} = \dfrac{100 * 78}{3600} =$	2.17	$a_{RT}^{max} = 6$
C	110	**Overflow queue-HCM**	$1.8145 \simeq$	
g/C	0.291	**Overflow queue-Markov Chain**	0	

Step 4- Calculate the probability of blockage (*Pattern 3*) for each *N*.

$$P(unacceptable \quad blockage) = P(Pattern \quad 3)$$

$$= \sum_{X_T=N+1-E(q)}^{a_T^{max}} \sum_{X_R=0}^{a_R^{max}} \frac{(\lambda_T)^{X_T} e^{-\lambda_T}}{X_T!} \frac{(\lambda_R)^{X_R} e^{-\lambda R}}{X_R!} \times \left[1 - \frac{\dbinom{N+1-E(q)+X_R}{X_R}}{\dbinom{X_T-E(q)+X_R}{X_R}} \right]$$

The results are summarized in table A-2. The results using the Markov Chain model also presented in Table A-3. The blockage probabilities obtained by using the HCM method and Markov Chain model to calculate the overflow queue are compared in Figure A-2.

TABLE A-2 Probability of Blockage Obtained with Residual Queues from the HCM Method

N	$P_{unacceptable\ Blockage}$	$P_{non\text{-}blockage}$	$P_{acceptable\ Blockage}$	$1 - (P_{non\text{-}blockage} + P_{acceptable\ Blockage})$
0	1.00	0.00	0.00	1.00
1	1.00	0.00	0.00	1.00
2	0.84	0.00	0.15	0.85
3	0.79	0.00	0.20	0.80
4	0.72	0.01	0.26	0.73
5	0.64	0.03	0.32	0.65
6	0.55	0.07	0.37	0.56
7	0.45	0.14	0.41	0.46
8	0.35	0.24	0.41	0.36
9	0.26	0.36	0.37	0.27
10	0.18	0.50	0.32	0.19
11	0.12	0.63	0.25	0.12
12	0.07	0.74	0.18	0.08
13	0.04	0.83	0.12	0.05
14	0.02	0.89	0.08	0.03
15	0.01	0.94	0.04	0.02
16	0.01	0.96	0.02	0.01
17	0.00	0.98	0.01	0.01
18	0.00	0.99	0.01	0.01
19	0.00	0.99	0.00	0.01
20	0.00	0.99	0.00	0.01

TABLE A-3 Probability of Blockage Obtained with Residual Queues from the Markov Chain Model

N	$P_{\text{unacceptable Blockage}}$	$P_{\text{non-blockage}}$	$P_{\text{acceptable Blockage}}$	$1-(P_{\text{non-blockage}}+P_{\text{acceptable Blockage}})$
0	0.84	0.00	0.15	0.85
1	0.79	0.00	0.20	0.80
2	0.72	0.01	0.26	0.73
3	0.64	0.03	0.32	0.65
4	0.55	0.07	0.37	0.56
5	0.45	0.14	0.41	0.46
6	0.35	0.24	0.41	0.36
7	0.26	0.36	0.37	0.27
8	0.18	0.50	0.32	0.19
9	0.12	0.63	0.25	0.12
10	0.07	0.74	0.18	0.08
11	0.04	0.83	0.12	0.05
12	0.02	0.89	0.08	0.03
13	0.01	0.94	0.04	0.02
14	0.01	0.96	0.02	0.01
15	0.00	0.98	0.01	0.01
16	0.00	0.99	0.01	0.01
17	0.00	0.99	0.00	0.01
18	0.00	0.99	0.00	0.01
19	0.00	0.99	0.00	0.01
20	0.00	0.99	0.00	0.01
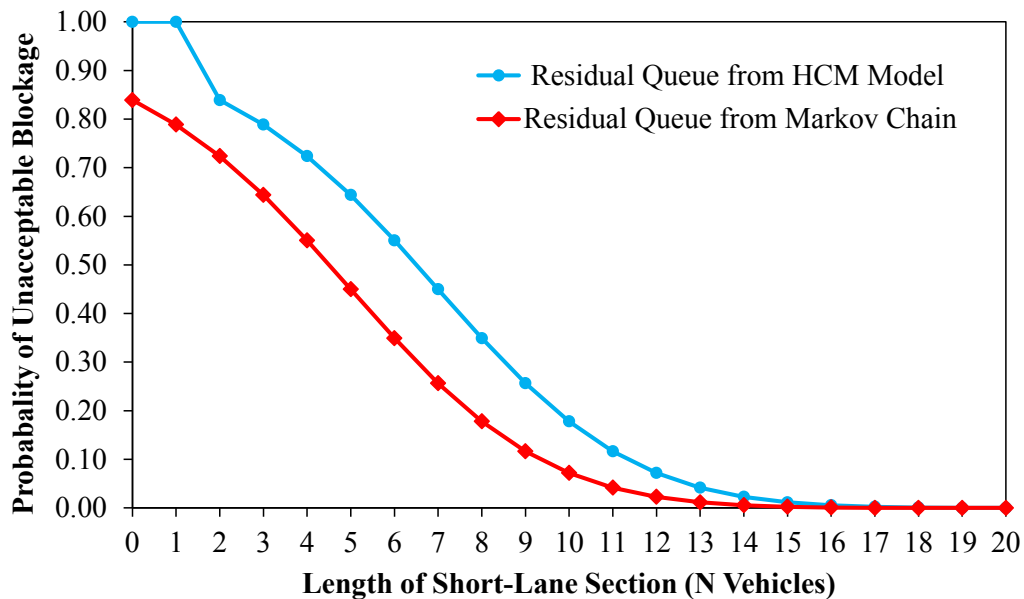
Figure A-2 Comparison of Two Blockage Probabilities Obtained with Residual queues from the HCM method and Markov Chain Model

Step 5- Calculate the blockage and non-blockage capacities for each N.

For $N=3$:

$$c_{block} = \frac{3600}{C}(N+1)\left(1+\frac{V_R}{V_T}\right) + \frac{g-g_1}{C}s_N = \frac{3600}{C}(3+1)\left(1+\frac{100}{400}\right) + \frac{32-8.96}{110}2014 = 585.54 \text{vph}$$

$$c_{non-block} = \frac{g}{C}s_N + \frac{r}{C}s_R = \frac{32}{110}2014 + \frac{78}{110}1565 = 1695.62 \text{vph}$$

$$c = P_{block}c_{block} + (1-P_{block})c_{non-block} = 0.79 \times 585.89 + 0.21 \times 1695.62 = 820.10 \text{vph}$$

The capacity results for different short-lane section lengths are calculated and summarized in Table A-4.

The random delay component which is dependent on the approach capacity is obtained following the HCM method:

$$d_2 = 900T\left[(X_L-1) + \sqrt{(X_L-1)^2 + \frac{8kIX_L}{c_LT}}\right]$$

$$= 900 \times 0.25\left[(0.62-1) + \sqrt{(0.62-1)^2 + \frac{8 \times 0.5 \times 1 \times 0.62}{801.28 \times 0.25}}\right] = 3.65 \text{sec}$$

The random delay is calculated for each N and summarized in the last column of Table A-4.

TABLE A-4 Approach Capacity and Random Delay Component Determined based on the Proposed Capacity Model and HCM Methodology

N	g_1	P_{block}	c_{block}	$c_{non-block}$	c	V/c	d_2
3	8.96	0.79	585.54	1695.62	820.10	0.61	**3.36**
4	10.70	0.72	594.61	1695.62	898.62	0.56	2.48
5	12.43	0.64	603.68	1695.62	992.65	0.50	1.83
6	14.17	0.55	612.74	1695.62	1099.38	0.45	1.36
7	15.91	0.45	621.81	1695.62	1212.60	0.41	1.04
8	17.65	0.35	630.88	1695.62	1323.86	0.38	0.82
9	19.39	0.26	639.94	1695.62	1424.80	0.35	0.68
10	21.13	0.18	649.01	1695.62	1509.32	0.33	0.59
11	22.87	0.12	658.08	1695.62	1574.75	0.32	0.53
12	24.61	0.07	667.15	1695.62	1621.72	0.31	0.49
13	26.35	0.04	676.21	1695.62	1653.07	0.30	0.47
14	28.09	0.02	685.28	1695.62	1672.59	0.30	0.46
15	29.83	0.01	694.35	1695.62	1683.96	0.30	0.45

Step 6- Calculate the approach uniform delay based on the arrival scenarios associated with the non-blockage and blockage conditions.

For *N=3*, when the through arrivals in red are less than or equal to three, no blockage will occur, otherwise through vehicles will block the right-turn channel entrance. For example, when one vehicle arrives in red, no blockage occurs, so:

$$V_{TH} = \frac{X_{TH} \times 3600}{r} = \frac{1 \times 3600}{78} = 46.15 \text{vph}$$

$$g_0 = \frac{V_{TH} \times r}{s_T - V_{TH}} = \frac{46.15 \times 78}{2070 - 46.15} = 1.78$$

$$D_{unblock}(1) = \frac{1}{2}[\frac{V_{TH}}{3600}(r + g_0)r] = \frac{1}{2}[\frac{46.15}{3600}(78 + 1.78)78] = 39.89 \text{sec}$$

$$d_{unblock}(1) = \frac{D_{unblock}(1)}{\dfrac{V_i}{3600}C} = \frac{39.89}{\dfrac{1.25 \times 46.15}{3600} \times 110} = 22.63 \, \text{sec}/_{veh}$$

$$P(1) = P(X_{TH} = 1) = \frac{(\lambda_T)^{X_{TH}} e^{-\lambda_T}}{X_{TH}!} = \frac{(8.67)^1 e^{-8.67}}{1!} = 0.0015 \qquad i = 1, 2, \ldots, 18(a_T^{\max})$$

When six vehicles arrive in red, a blockage occurs by arrival of three vehicles ($X=3$) beyond the channel throat, so:

$$V_{TH} = \frac{X_{TH} \times 3600}{r} = \frac{6 \times 3600}{78} = 295.38 \, \text{vph}$$

$$t_1 = \frac{(N+1) \times r \times p_t^{-1}}{X + p_t^{-1} \times (N+1)} = \frac{(3+1) \times 78 \times 0.8^{-1}}{2 + 0.8^{-1} \times (3+1)} = 55.71 \, \text{sec}$$

$$g_1 = \frac{N+1}{s_T} \times 3600 + t_s = \frac{3+1}{2070} \times 3600 + 2 = 8.96 \, \text{sec}$$

$$t_2 = \begin{cases} \dfrac{V \times (r - t_1 + g_1)}{s_N - V} = \dfrac{1.25 \times 295.38 \times (78 - 48.75 + 8.96)}{2014 - 1.25 \times 295.38} = 8.58 & t_2 \leq g - g_1 \\ g - g_1 & otherwise \end{cases}$$

$$D_{block}(i) = \frac{1}{2}(N+1)t_1 + (N+1)(r - t_1) + \frac{1}{2}(N+1)g_1 + \frac{1}{2}[\frac{V}{3600}(r - t_1 + t_2 + g_1)^2 - s_N t_2^2]$$

$$= \frac{1}{2}(3+1) \times 55.71 + (3+1)(78 - 55.71) + \frac{1}{2}(3+1) \times 8.96$$

$$+ \frac{1}{2}[\frac{1.25 \times 295.38}{3600}(78 - 55.71 + 8.58 + 8.96)^2 - 2014 \times 8.96^2]$$

$$= 324.08 \, \text{sec}$$

$$d_{block}(6) = \frac{D_{block}(6)}{\dfrac{V_i}{3600}C} = \frac{324.08}{\dfrac{1.25 \times 295.38}{3600} \times 110} = 28.73 \, \text{sec}/_{veh}$$

$$P(6) = P(X_{TH} = 6) = \frac{(\lambda_T)^{X_{TH}} e^{-\lambda_T}}{X_{TH}!} = \frac{(8.67)^6 e^{-8.67}}{6!} = 0.1000 \qquad i = 1, 2, \ldots, 18(a_T^{\max})$$

For each arrival scenario, the above process is repeated to finally obtain the uniform approach delay:

$$d_1 = \sum_{i=1}^{3} d_{unblock}(i) \times P(i) + \sum_{i=3}^{18} d_{block}(i) \times P(i)$$

For the case that $N=3$, the approach uniform delay is obtained 32.48 seconds as illustrated in Table A-5.

TABLE A-5 Approach Delay Calculated based on the Proposed Model for $N=3$

No. of Through Vehicles Arrive in Red, $i = X_{TH}$	Equivalent Through Volume	t	g	Total Uniform Delay		Probability of X_{TH} Arrivals in Red	Probable Average Uniform Delay
Non-Blockage Condition							
X_{TH}	V_{TH}		g_0	$D_{unblock}(i)$	$d_{unblock}(i)$	$P(i)$	$P(i) \times d_{unblock}(i)$
1	46.15		1.78	39.89	22.63	0.00	0.03
2	92.31		3.64	81.64	23.16	0.01	0.15
3	138.46		5.59	125.39	23.71	0.02	0.44
Blockage Condition							
X_{TH}	V_{TH}	t_1	g_1	$D_{block}(i)$	$d_{block}(i)$	$P(i)$	$P(i) \times d_{block}(i)$
4	221.54	65.00	8.96	221.41	26.17	0.04	1.06
5	258.46	55.71	8.96	270.65	27.42	0.07	1.92
6	295.38	48.75	8.96	324.08	28.72	0.10	2.91
7	332.31	43.33	8.96	381.56	30.06	0.13	3.77
8	369.23	39.00	8.96	443.17	31.42	0.14	4.27
9	406.15	35.45	8.96	509.07	32.82	0.13	4.30
10	443.08	32.50	8.96	579.56	34.25	0.11	3.89
11	480.00	30.00	8.96	654.71	35.71	0.09	3.19
12	516.92	27.86	8.96	731.21	37.04	0.06	2.39
13	553.85	26.00	8.96	807.84	38.19	0.04	1.64
14	590.77	24.38	8.96	884.59	39.20	0.03	1.04
15	627.69	22.94	8.96	961.44	40.10	0.02	0.62
16	664.62	21.67	8.96	1038.37	40.91	0.01	0.34
17	701.54	20.53	8.96	1115.36	41.63	0.00	0.18
Approach Uniform Delay=d							32.30

Step 7- Calculate the approach control delay.

$$d = d_1 + d_2$$

For *N=3*:

$$d = 32.30 + 3.36 = 35.66 \sec$$

The results for different short-lane section lengths are shown in Table A-6. The results from VISSIM also are presented in this table.

To see how the model results are different from the simulation outputs, the error for each length scenario is obtained using the following equation:

$$\text{error} = \frac{\left| d_{Model}(N) - d_{VISSIM}(N) \right|}{d_{Model}(N)} = \frac{\left| 35.66 - 37.10 \right|}{35.66} = 0.04 \qquad N = 3$$

TABLE A-6 Estimated Approach Control Delay

N	VISSIM	Model			error
		d_2	d_1	$d = d_1 + d_2$	
3	37.10	3.36	32.30	35.66	0.04
4	35.67	2.48	31.55	34.03	0.05
5	34.92	1.83	30.89	32.72	0.07
6	33.92	1.36	30.3	31.66	0.07
7	32.26	1.04	29.76	30.80	0.05
8	31.12	0.82	29.26	30.08	0.03
9	30.35	0.68	28.8	29.48	0.03
10	29.97	0.59	28.41	29.00	0.03
11	29.78	0.53	28.1	28.63	0.04
12	29.52	0.49	27.87	28.36	0.04
13	29.36	0.47	27.74	28.21	0.04
14	29.18	0.46	27.63	28.09	0.04
15	29.05	0.45	27.57	28.02	0.04
				ME	**0.04**

The mean error (ME) for the defined volume scenario ($V_T = 400\text{vph}, V_R = 100\text{vph}$)

and signal timing ($C = 110\sec, g = 32\sec$) is calculated from:

$$ME = \frac{1}{n} \sum_{N=3}^{15} \frac{\left|d_{Model}(N) - d_{VISSIM}(N)\right|}{d_{Model}(N)}$$

The approach delay estimated from the proposed model is illustrated in Figure A-3 as
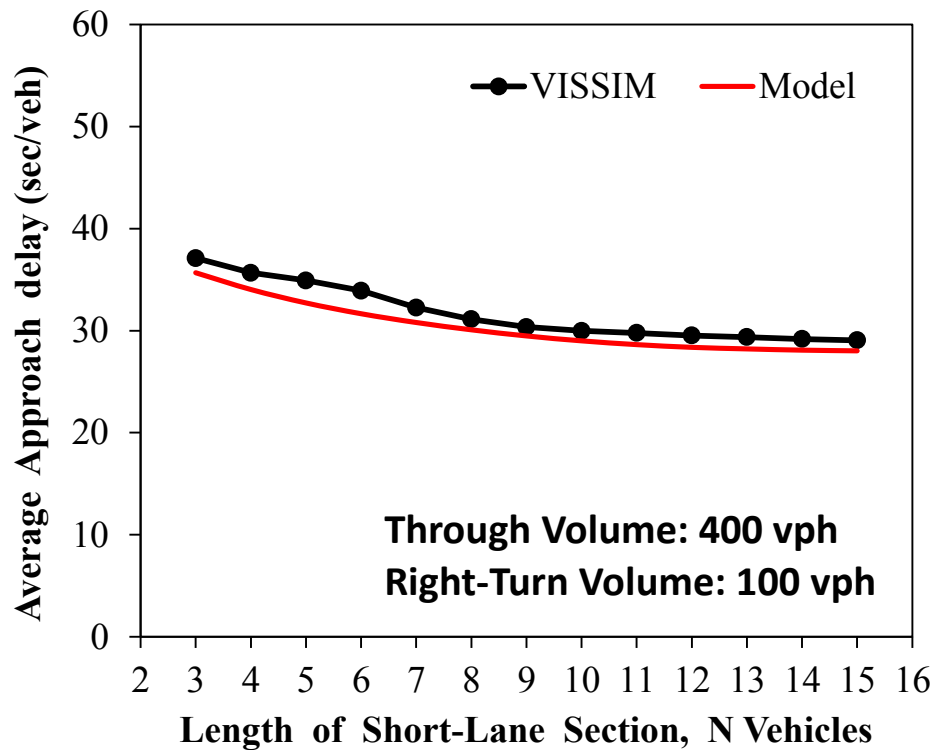
well as the simulation results.

Figure A-3 Approach Control Delay from VISSSIM and the Proposed Model